Solvent-Controlled Intramolecular Electron Transfer in Ionic Liquids

ARTICLE *in* THE JOURNAL OF PHYSICAL CHEMISTRY B · MAY 2011

Impact Factor: 3.3 · DOI: 10.1021/jp200339e · Source: PubMed

5 AUTHORS, INCLUDING:

Min Liang
Pennsylvania State University
9 PUBLICATIONS **242** CITATIONS

SEE PROFILE

Mark Maroncelli
Pennsylvania State University
126 PUBLICATIONS **11,750** CITATIONS

SEE PROFILE

THE JOURNAL OF PHYSICAL CHEMISTRY B

ARTICLE

pubs.acs.org/JPCB

Solvent-Controlled Intramolecular Electron Transfer in Ionic Liquids

Xiang Li, Min Liang, Anjan Chakraborty,† Minako Kondo, and Mark Maroncelli*

Department of Chemistry, The Pennsylvania State University, University Park, Pennsylvania 16802, United States

Supporting Information

ABSTRACT: The rates of excited-state intramolecular electron transfer in 9-(4-biphenyl)-10-methylacridinium ($BPAc^+$), crystal violet lactone (CVL), and bianthryl have been measured in a variety of ionic liquids using time-correlated single-photon counting. All three of these reactions had previously been studied in conventional dipolar solvents and their reaction rates shown to be controlled by solvation dynamics. The main focus of this work is to ask whether the same relationships between reaction and solvation times already established in dipolar solvents also apply in ionic liquids. In $BPAc^+$, where reaction conforms to a simple two-state kinetic scheme and reaction rates are easily measured, the result is a clear "yes". In the case of bianthryl, whose spectra reflect the more complex kinetics of a barrierless process, the answer is also yes. In contrast to other recent studies of bianthryl, the present results demonstrate that the same equality between (integral) reaction times and solvation times observed in conventional solvents also applies in ionic liquids. Finally, the case of CVL is less clear due to the greater uncertainty associated with the data afforded by this weak fluorophore, combined with a lack of data in conventional solvents having large solvation times. But the CVL reaction can also be reasonably interpreted as exhibiting a common behavior in dipolar and ionic solvents.

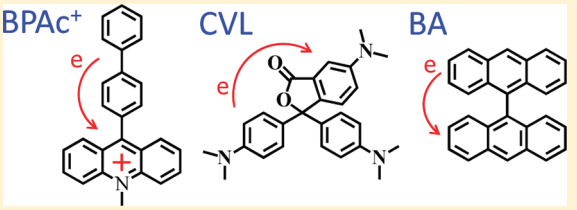

1. INTRODUCTION

Room-temperature ionic liquids (ILs) are an emerging class of materials currently being explored in a variety of contexts.[1−6] In many applications, such as their use as solvents for organic synthesis[1,7−9] and in electrochemical processes,[10,11] it is important to understand how electron transfer might be affected by the purely ionic environment presented by these liquids. In particular, one would like to know whether ionic liquids are in some way distinctive in their influence on electron-transfer reactions or whether solvent effects are qualitatively the same as in the well-studied case of high-polarity conventional solvents. In this paper we address one aspect of this question, whether the relationship between solvation and reaction times in three intramolecular charge-transfer reactions known to be solvent controlled in dipolar solvents extends to the longer solvation times existent in ionic liquids.

As far as energetic aspects of electron transfer are concerned, there appears to be little to distinguish ionic liquids from dipolar solvents of high polarity. For example, Lynden-Bell[12] used molecular dynamics simulations of two model dimethylimidazolium ionic liquids to investigate the extent to which the usual Marcus-type descriptions of solvation energies are applicable. Just as in the case of dipolar liquids, she found that the free energy profiles associated with one-electron oxidation and reduction of spherical ions closely conform to the parabolic shape expected by Marcus theory. More remarkably, Lynden-Bell also observed the reorganization and activation energies and even the charge dependence of these quantities to be nearly the same in the ionic liquids and in acetonitrile, the simulators' default choice of comparison dipolar solvent. Similar observations were made in an independent study by Shim and Kim,[13] who simulated charge transfer between two atoms of a model diatomic solute in 1-ethyl-3-methylimidazolium hexafluorophosphate. These two simulations, together with extensive evidence from solvatochromic studies of ionic liquids,[14,15] including some direct measurements of energies associated with charge-transfer transitions,[16,17] suggest that there is little to distinguish solvation energies in an ionic liquid environment from those found in highly polar conventional solvents such as acetonitrile and dimethyl sulfoxide.

This energetic similarity might not be expected to extend to dynamical solvent effects on electron transfer,[18] given the very different time scales and distinct mechanisms of solvation in ionic liquids compared to dipolar solvents. As a result of their much higher viscosities, the solvation response in ionic liquids is hundreds of times slower than in most conventional solvents.[19,20,17] In addition, the response is broadly distributed in time, with significant contributions from components ranging from sub-picosecond to nanosecond time scales.[20] Finally, simulation studies have shown that, in contrast to the predominantly rotational response of dipolar solvents, the primary means of relaxing the solvation energy in ionic liquids is translational motion of ions.[21,22] These differences might well be expected to produce both quantitative and qualitative differences in electron-transfer processes susceptible to dynamical solvent influence. To explore this possibility, Shim and Kim used simulations of electron transfer in a model diatomic solute in two different ionic liquids to investigate how

Received: January 12, 2011
Revised: April 3, 2011
Published: May 02, 2011

friction on barrier-crossing and well dynamics might influence adiabatic electron-transfer reactions.[13,23] They again compared the behavior in the ionic liquids to that in acetonitrile. For high-barrier (>10 k_BT) reactions, these authors found only moderate deviations (factors of 3−5) from transition state theory predictions and these deviations were well-described by the Grote−Hynes theory.[24] In the cases examined, the dynamical solvent effects on the electron transfer were found to be virtually identical in the ionic liquid and acetonitrile, despite the nearly 100-fold difference in the viscosities or zero-frequency friction in the two solvents. This similarity results from the fact that for high-barrier reactions only the higher frequency portions of the solvent friction, those coming from the ultrafast components of the solvation response, are relevant, and this fast portion of the friction is comparable in the acetonitrile and ionic liquid models. Only for reactions with lower barriers, where more of the full friction is felt during barrier crossing and where well dynamics become important, did they predict much larger dynamical solvent effects and large differences between the ionic liquids and acetonitrile.[23]

A variety of experimental studies of electron-transfer rates have also been performed. Many of these studies involved diffusion-limited bimolecular electron-transfer reactions.[25−32] In a number of cases, reaction rates were reported to be much greater than predicted on the basis of simple viscosity scaling of the rates observed in conventional solvents. Our analysis suggests that these faster-than-expected rates are probably due to the inapplicability of the simplest treatments of diffusion-limited reaction in high-viscosity liquids rather than to unusual behavior of the electron-transfer process itself.[33,34] Electrochemical methods have also been used to measure heterogeneous electron-transfer kinetics in a variety of ionic liquids.[10,35] Of most interest in the present context are experiments of van Eldik and co-workers[36,37] who used cyclic voltammetry to measure electron-transfer rates of the ferrocene/ferrocinium couple on bare gold[36] and on alkanethiol-coated[37] electrodes in 1-butyl-3-methylimidazolium bis(trifluoromethylsulfonyl)imide ($[Im_{41}][Tf_2N]$). The observed rates were interpreted in terms of a transition from the regimes of solvent-controlled adiabatic electron transfer on bare electrodes[36] to nonadiabatic electron transfer as a function of the alkanethiol chain length.[37] A complicating factor in fully interpreting these and other heterogeneous electron-transfer rates is the fact that ionic liquids bind strongly to solid surfaces and form multilayer structures that are only now beginning to be understood.[38,39] Virtually nothing is known about solvation dynamics within these layers.

Intramolecular electron-transfer reactions, typically photoinduced, afford information that can be more readily interpreted in terms of dynamical solvent effects. Relatively few experiments of this sort have so far been performed in ionic liquids.[40−53] Of the studies published to date, several bear on the question of how the slow solvation dynamics in ionic liquids affects electron transfer. In addition to studies of crystal violet lactone[41,42,51] and bianthryl[45−47] to be discussed in more detail below, studies of two other electron-transfer reactions should be mentioned. Lockard and Wasielewski[40] used femtosecond transient absorption to measure charge separation and recombination rates in a covalently linked organic donor−acceptor dyad in several conventional solvents and in an imidazolium ionic liquid. At room temperature, these reactions were observed to take place on comparable time scales (1−50 ps) in dipolar solvents and the ionic liquid, suggesting that the much slower solvation in the ionic liquid had little effect on these reactions. They also observed a clear difference in the temperature dependence of the rate of the recombination reaction, which might signal partial solvent control or might instead be related to the viscosity affecting conformational dynamics also thought to be relevant. In similar experiments, Vauthey and co-workers[44] reported electron-transfer times in the covalently linked perylene−dimethylaniline dyad (PeDMA) in six dipolar solvents and in 3-ethyl-1-methylimidazolium ethyl sulfate. They noted that much slower and highly nonexponential charge separation occurs in the ionic liquid compared to the conventional solvents studied. In the latter solvents, the electron transfer was observed to be approximately equal to solvation times measured with coumarin 153.[54] On the basis of an estimated solvation time in the ionic liquid, we find that roughly the same equality of electron-transfer and solvation time appears to hold for the ionic liquid as well. In this respect, the PeDMA reaction bears some resemblance to the bianthryl reaction studied here.

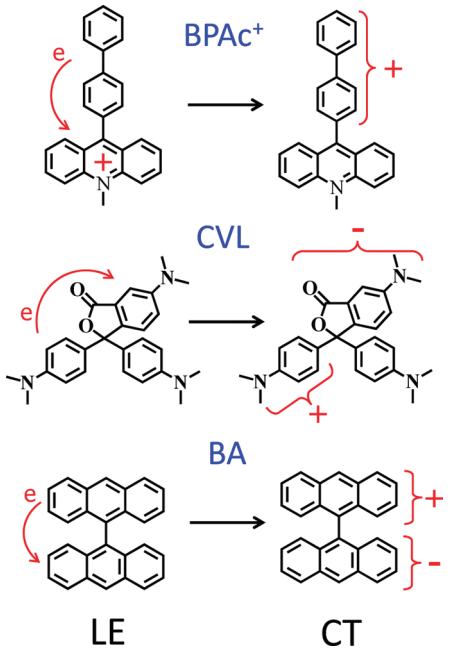

Figure 1. Schematic of the charge-transfer processes in 9-(4-biphenyl)-10-methylacridinium ($BPAc^+$), crystal violet lactone (CVL), and bianthryl (BA).

In the present work we use picosecond time-resolved emission spectroscopy to measure intramolecular electron-transfer rates in the three solutes 9-(4-biphenyl)-10-methylacridinium ($BPAc^+$), crystal violet lactone (CVL), and bianthryl (BA) (Figure 1). All three solutes have been previously characterized in conventional solvents, where it has been shown that the electron-transfer processes in Figure 1 are primarily controlled by solvation dynamics. Observation of solvent control suggests that these reactions can be viewed as adiabatic processes on reaction coordinates which are dominated by solvent degrees of freedom rather than intramolecular modes. (See ref 18 for a helpful summary of the various possibilities that exist for solvent control of electron-transfer processes.) The reactions chosen share a number of common features. First, all three solutes exhibit dual fluorescence whose composition varies with solvent polarity. In low-polarity solvents, emission occurs primarily from a "locally excited" or LE state reached by excitation in the lowest energy

absorption band. The term "local" here is used to indicate that excitation can be thought of as residing on one portion of the molecule: the acridinium ring in the case of $BPAc^+$, the aminophthalide ring in CVL, and one of the two anthracene rings in bianthryl.[55] In high-polarity solvents, emission from a "charge-transfer" (CT) electronic state is also observed, and this emission typically dominates the spectrum. In all three cases, the LE → CT conversion entails charge re-distribution which amounts to transfer of approximately one electron in the directions indicated in Figure 1. In most conventional solvents, the LE → CT reaction and its reverse are rapid relative to depopulation of the excited state, so that the relative amounts of LE and CT emission reflect the equilibrium between these states. Finally, in all three cases this equilibrium shifts strongly in favor of the CT state with increasing solvent polarity. More background on the individual reactions is now provided.

$BPAc^+$ is one of a series of fluorescent donor-substituted acridinium molecules introduced by Jones and co-workers[56] for studying electron-transfer reactions having variable driving force.[57−60] Horng et al.[58] measured the time-resolved emission of $BPAc^+$ in 21 conventional solvents at 25 °C. Predominantly biexponential kinetics with widely separated time constants conforming to expectations for a two-state reaction were observed. The shorter time constant, which ranged between 4 and 500 ps, could be associated with the LE → CT reaction time. In 14 solvents more polar than acetone, Horng et al. observed a strong correlation between this reaction time (τ_{rxn}) and solvation times $\langle\tau_{solv}\rangle$ measured with the nonreactive solute coumarin 153 (C153). This relationship could be approximately expressed $\tau_{rxn} \cong 8.4\langle\tau_{solv}\rangle^{0.65}$. No measurements of $BPAc^+$ or related molecules in ionic liquids have been reported previously.

CVL is a molecule whose dual fluorescence was characterized only recently in an extensive study by Karpiuk,[61] with additional contributions from our group.[62] On the basis of the spectra and dynamics of the component chromophores of CVL,[63,64] Karpiuk concluded that the LE state entails excitation of the aminophthalide portion of the molecule, whereas the CT state is one in which an electron has transferred from one or both dimethylamino fragments to the aminophthalide ring (Figure 1). Using an analysis of the solvatochromism of the two emission bands, Karpiuk estimated dipole moments of ∼11 D for the LE state and ∼25 D for the CT state,[61] which can be compared to a dipole moment of 6.0 D [62] in the ground state. As these dipole moments indicate, the LE state already entails a significant charge redistribution compared to the ground state, which renders both the LE and CT emission significantly solvatochromic. Li and Maroncelli[62] measured the time-resolved emission of CVL in a range of solvents and, as in the case of $BPAc^+$, found primarily well-resolved biexponential kinetics with a short time constant of 10−100 ps due to reaction and a long time constant in the 1−20 ns range. They used information from both emission decays and LE/CT contributions to the steady-state emission spectra to deduce the driving force for the LE → CT reaction, which was found to vary from about −15 kJ/mol in nonpolar solvents to +10 kJ/mol in highly polar solvents. On the basis of transient absorption data in three solvents, Karpiuk and co-workers[65] suggested that the charge-transfer reaction in CVL is controlled by solvation dynamics. A more extensive survey of reaction kinetics in a number of solvents and solvent mixtures[62] supported this suggestion, but the distinction between control by solvation dynamics as oppose to other frictional effects could not be as definitively established in CVL as the other two solutes studied here, because an additional nonradiative channel[61] precluded measurement of the reaction rate in protic solvents.[62]

CVL has also been studied in ionic liquids.[41,42,51,66] Jin et al.[41] reported a large variation of the relative intensities of the LE and CT bands in the steady-state spectra of CVL with excitation wavelength, and interpreted this variation as an example of dynamic heterogeneity in ionic liquids. Annapureddy and Margulis[66] performed simulations of the experimental system studied by Jin et al. They showed that the sluggish dynamics in ionic liquids is such that site-to-site variations in solvation energies can persist for several nanoseconds and that this persistence should result in excitation dependence of both fluorescence spectra[67] and excited-state electron-transfer rates.[66] During the course of the experiments reported in the present study we have found that the large variations in the steady-state emission spectra reported by Jin et al.[41] were spurious, probably as a result of solvent impurity emission contaminating the relatively weak emission of CVL.[42] We have checked for excitation wavelength dependence in a number of the solute + ionic liquid combinations reported here and find only very small variations to LE/CT intensity ratios. Although we believe that these variations are genuine, better examples have been reported using other reactions,[33,68,50] so we do not discuss this phenomenon further here.

A final study of CVL in ionic liquids was recently reported by Santhosh and Samanta.[51] These authors measured steady-state spectra and several photophysical properties of CVL in six ionic liquids as well as complete time-resolved emission spectra in one liquid at room temperature. They observed a good correlation between the frequency of the LE emission and the $E_T(30)$ polarity parameter[15] and also noted much lower emission quantum yields in 1-alkyl-3-methylimidazolium ionic liquids compared to other ionic liquids studied. From these observations they concluded that the hydrogen bond donating ability of the C(2)−H atom in the former liquids is sufficient to open the additional deactivation channel described by Karpiuk for CVL in alcohol solvents.[61] In the ionic liquid 1-butyl-2,3-dimethylimidazolium bis(trifluoromethanesolufonyl)imide, Santhosh and Samanta reported an isoemissive point in the area-normalized spectra and a rise time of the CT emission (1 ns) which was comparable in magnitude to the solvation time they measured in this liquid using C153 (690 ps). On this basis they suggested that the LE → CT reaction is also controlled by solvation dynamics in ionic liquids.

Bianthryl has enjoyed much greater study than the other two solutes used in the present work. Schneider and Lippert[69] first recognized charge transfer to be responsible for the dual fluorescence of bianthryl. They estimated excited-state dipole moments of 18 D in polar solvents, consistent with a full electron transfer between the two anthracene chromophores. Since that seminal work numerous groups have studied various aspects of the excited-state behavior of bianthryl in conventional solvents[70−84] and in the gas phase,[85,86] leading to a rich, but not entirely consistent, description of the LE → CT reaction. Pioneering measurements and modeling of the time-resolved emission of bianthryl in polar solvents were performed by Barbara and co-workers roughly 20 years ago.[70−73] They postulated that the excited-state charge transfer in bianthryl could be described in terms of an adiabatic process on a single S_1 potential energy surface produced via the mixing of three diabatic states: an LE state consisting of an excitonic mixture AA*↔A*A and a pair of CT states, A^+A^- and A^-A^+.[55] On the basis of the near equality observed between the

electron-transfer times of bianthryl and solvation times measured with coumarin probes,[70] they further proposed that the reaction coordinate was comprised solely of solvent polarization modes. Using this description, they were able to provide a coherent account of the solvent dependence of the steady-state emission of bianthryl and the time-dependent emission observed in high-polarity solvents.[72,73] In propylene carbonate for example, their modeling suggested that the Franck−Condon (FC) region is predominantly of LE character, but that there exists only a small ($\sim k_BT$) energy barrier to transfer to the CT region of S_1, whose minimum lies below the FC region by about 21 kJ/mol.[73] The highly nonexponential reaction kinetics they observed experimentally and its resemblance to the time dependence of the dynamic Stokes shift was explained by the very small barrier and the nonexponential survival probability of LE character on such a surface. This complex reaction kinetics in bianthryl contrasts with the simple two-state type of kinetics observed in $BPAc^+$ and CVL in conventional solvents. But it is also reasonable to describe these latter reactions using a one-dimensional adiabatic description similar to the one envisioned for bianthryl. In these cases the reaction barrier must be larger than in bianthryl in order to more effectively separate populations into LE and CT regions of the potential. If such a description is correct, analyses of the sort described by Shim and Kim[23] require that in all three cases the barrier must be quite small, no more than a few k_BT to be consistent with the observed dependence on solvation times.

It should be noted that subsequent work on bianthryl suggests that the model proposed by Barbara and co-workers[72,73] is not a complete description of this reaction. For example, torsional dynamics are neglected in the model, and such dynamics are likely to play some role in determining the details of the spectral dynamics observed.[74,75,85] There also is some discrepancy between the LE−CT equilibrium constants deduced from fluorescence measurements and determinations of dipole moments in weakly polar solvents[78] as well as with equilibrium constants deduced from transient absorption (TA) measurements in high-polarity solvents.[82] This discrepancy has yet to be resolved. Finally, the most recent femtosecond TA studies indicate that there is some CT[82] or "pre-CT"[83] state population already present at times of less than 50 fs, something not anticipated by Barbara's photodynamic model as originally proposed. These observations suggest that refinement, probably incorporation of coordinates other than solvation into the model, will be required for a completely quantitative description of the bianthryl reaction.

Bianthryl has been studied in ionic liquids using both picosecond time-resolved emission[45−47] and transient absorption on femtosecond[45] and nanosecond[45,84] time scales. Nagasawa and co-workers[45] measured femtosecond broadband TA in the visible region and time-resolved emission spectra of bianthryl in imidazolium ionic liquids. The TA measurements revealed rise times of an excited-state absorption attributed to the CT state in the range of 53−100 ps.[45] Emission spectra recorded with 30 ps resolution were used to monitor the dynamic Stokes shift of the CT band of bianthryl in these same solvents. The fact that the emission Stokes shifts extended to times much longer than the CT rise observed in TA experiments led Nagasawa et al.[45] to conclude that the LE → CT reaction proceeds on a different time scale from solvation in ionic liquids. This conclusion implies that a different relationship exists between solvation and reaction in ionic liquids compared to conventional solvents, where approximate equality between the times prevails.[71,72,82] Independent measurements of the time-resolved emission spectra of bianrthyl in the same three ionic liquids were reported by Samanta and co-workers.[47] These authors estimated the LE → CT reaction time from the decay observed near the peak of the LE emission and measured solvation times in terms of the dynamic Stokes shift of the entire emission band. They found the former times to be significantly smaller than the latter times and again concluded that reaction and solvation occur on different time scales in ionic liquids.[47] In a second study, Nagasawa and co-workers used the dynamic Stokes shift of the bianthryl spectrum to measure the temperature dependence of the solvation response in five ionic liquids. They observed a good correlation between the average solvation times measured in this way and the solvent viscosity in most of these liquids. The dependence upon viscosity was weaker ($\langle\tau_{solv}\rangle \propto \eta^{0.60}$) than was previously observed using C153 as a solvation probe ($\langle\tau_{solv}\rangle \propto (\eta/T)^{1.0}$).[17]

In the present work we measure reaction times of intramolecular electron transfer in $BPAc^+$, CVL, and bianthryl in an assortment of ionic liquids. We do not attempt to model the connection between solvation dynamics and reaction here. Instead, we merely compare the reaction times measured in ionic liquids to solvation times measured with C153 in these same liquids and ask whether the relationships previously established in dipolar solvents extend to ionic liquid solvents. The answer we obtain is a definite yes in the cases of $BPAc^+$ and bianthryl and a tentative yes in the case of CVL. Because the details of the methods used to deduce reaction times of these three reactions differ, we present the results of each solute separately. Where possible, we compare the results and conclusions provided here to prior ionic liquid work, in particular addressing the disagreement between the conclusions of the present study and those made in previous studies of the bianthryl reaction in ionic liquids.[45,47]

2. EXPERIMENTAL SECTION

9-(4-Biphenyl)-10-methylacridinium ($BPAc^+$) and 9-phenyl-10-methylacridinium (PAc^+) hexafluorophosphate were prepared by Jones as described in ref 87. Crystal violet lactone (CVL) was obtained from Sigma-Aldrich (97%) and recrystallized twice from acetone. 9,9′-Bianthracene (or bianthryl, BA) was prepared by the procedure of Bell and Waring[88] and recrystallized from carbon tetrachloride. In all cases purity was initially checked by thin layer chromatography and confirmed by lack of detectable impurity fluorescence.

Ionic liquids were obtained from a variety of sources. Unless otherwise specified these materials were used as received except for drying. 1-Ethyl-3-methylimidazolium bis(trifluoromethylsulfonyl)imide ($[Im_{21}][Tf_2N]$) and 1-butyl-3-methylimidazolium tetrafluoroborate ($[Im_{41}][BF_4]$) were obtained from Iolitec (99%). $[Im_{41}][BF_4]$ was dissolved in methylene chloride and treated with activated carbon several times to remove fluorescent impurities. 1-Butyl-3-methylimidazolium hexafluorophostphate ($[Im_{41}][PF_6]$) was obtained from Covalent Associates (99+%) and propyltrimethylammonium bis(trifluoromethylsulfonyl)-imide ($[N_{3111}][T_2fN]$) from Kanto Chemical. Isopropyldimethyl bis(trifluoromethylsulfonyl)imide ($[N_{ip311}][Tf_2N]$), 1-propyl-3-methylpyrrolidinium bis(trifluoromethylsulfonyl)imide ($[Pr_{31}]$-$[Tf_2N]$), and 1-butyl-3-methylpyrrolidinium bis(trifluoromethylsulfonyl)imide ($[Pr_{41}][Tf_2N]$) were prepared by Baker as described in ref 89a. Finally, tributyltetradecylphosphonium bis(trifluoromethylsulfonyl)imide ($[P_{14\,666}][Tf_2N]$) was prepared

from the chloride salt. Tributyltetradecylphosphonium chloride ($[P_{14\,666}][Cl]$; Cytec Canada) was first purified by washing twice with water, drying, and dissolving the dried liquid in dichloromethane (DCM) containing activated carbon. This mixture was stirred overnight and the carbon removed using a syringe filter. The DCM solution was then mixed with an approximately equimolar amount of aqueous lithium bis(trifluoromethylsulfonyl)imide and the reaction stirred overnight at room temperature. The DCM layer was separated and washed with water 10 or more times until no Cl^- could be detected with $AgNO_3$. DCM was removed from the final product by rotary evaporation for 1 h at 60 °C. All ionic liquid samples were dried on a vacuum line until the water content was below 200 ppm as determined by coulometric Karl Fischer titration.

Samples for steady-state spectroscopy were prepared in 1 cm quartz cuvettes at concentrations providing optical densities of less than 0.2 at the excitation wavelength. Absorption measurements were made using a Hitachi U-3000 UV/visible spectrophotometer with a resolution of 1 nm. Corrected emission spectra were recorded with either PTI Quanta-Master 1 or Spex Fluorolog 212 fluorimeters at 2 nm resolution. Solvent blanks were subtracted from all spectra and the spectra converted to a frequency representation prior to analysis. Low-temperature spectra were recorded using vacuum-sealed samples in an Oxford DN-1754 cryostat.

Time-resolved emission decays were collected using a time correlated single-photon counting (TCSPC) instrument whose main features have been previously described.[90] The excitation source was the doubled output of a cavity-dumped Ti:sapphire laser operating at a repetition rate of 5.4 MHz. Excitation wavelengths ranged between 370 and 420 nm depending on the solute. Samples were contained in 1 cm cuvettes into which a yellow filter glass was inserted to remove reflections near time zero. The optical densities of these samples were typically below 0.2 but sometimes as high as 0.4 in order to minimize the effects of impurity fluorescence from the ionic liquid solvents. Emission was collected at magic angle through an ISA H10 monochromator using an emission band pass of 8 nm. The overall response time of the TCSPC instrument was 25−30 ps (full width at half-maximum (fwhm)), as measured using a scattering solution. Data were collected over time windows of 6−30 ns, depending on the solute and its lifetime. Emission transients were fit using observed instrument response functions and an iterative reconvolution algorithm. In the case of CVL, whose fluorescence is weak, solvent blanks were recorded under identical conditions to those of the sample and these blank decays subtracted prior to data analysis. Emission transients at 15−25 wavelengths were collected and time-resolved spectra reconstructed from fits to these data using methods described in ref 91. Temperatures for the steady-state and TCSPC measurements were maintained to ±0.2 °C using water from a circulating bath.

Preliminary fluorescence upconversion measurements were made with the same laser source using 390 nm excitation. The collection optics and detection electronics were essentially identical to those described in previous work.[54] The only significant difference is that the prism pulse compressors were omitted. Samples were contained in a 1 mm thickness quartz flow cell connected to a peristaltic pump and the system purged with nitrogen at room temperature, 21 ± 1 °C. Emission was recorded at magic angle. The instrument response function of this system was ∼300 fs (fwhm) as judged by upconversion of the Raman signal from neat solvents.

3. RESULTS AND DISCUSSION

Before discussing the results obtained with different solutes, we pause to consider the ionic liquids used in this study. Because the experiments described here were carried out over the course of several years, a common set of solvents and conditions was not used for all three solutes. Instead, the choice of solvents was dictated by availability and by the need to use solvents of the highest optical purity possible, especially for the weakly fluorescent solute CVL. Table 1 lists the ionic liquids studied along with some properties pertinent to their use as solvents in charge-transfer contexts. (We specify cations here by type as Im = 1-alkyl-3-methylimidazolium, N = ammonium, Pr = pyrrolidinium, and P = phosphonium and use numerical subscripts to indicate the carbon numbers in *n*-alkyl groups or ip = isopropyl to indicate the variable substituents.) Some indicators of the ability to stabilize dipolar and charged species are provided by the bulk ion concentrations [IP] and the solvent reorganization energies λ_{C153} and free energy changes ΔG_{C153} associated with the $S_0 \leftrightarrow S_1$ transition of the solvatochromic probe coumarin 153 (C153).[17] The concentration of ions (defined here as ± pairs) has been suggested as a useful measure of solvent polarity in ionic liquids. Within the present collection of liquids the only significant variations from a value of ∼3 M occur in the liquids not based on the Tf_2N^- (bis(trifluoromethylsulfonyl)imide) anion and with the unusually large cation in $[P_{14\,666}][Tf_2N]$. The molecular measures of solvation energies provided by λ_{C153} and ΔG_{C153} are only weakly correlated to this bulk ion concentration. These latter measures indicate that solvation energetics should be reasonably constant among this collection of ionic liquids, except in the case of $[P_{14\,666}][Tf_2N]$. Such constancy is important because barrier heights and therefore rates of electron-transfer reactions could vary significantly with solvent polarity. The similar values of λ_{C153} and ΔG_{C153} measured in all but the $[P_{14\,666}][Tf_2N]$ solvent suggest that the primary determinant of variable reaction rates measured here will be variations solvent dynamics rather than energetic differences.

As a measure of solvation dynamics we use the integral time associated with the dynamic Stokes shift of C153

$$\langle \tau_{solv} \rangle = \int_0^\infty \{\nu(t) - \nu(\infty)\}\, dt / \{\nu(0) - \nu(\infty)\} \qquad (1)$$

where the $\nu(t)$ are frequencies directly measured using TCSPC. Due to time resolution limitations these solvation times are an upper limit to the true integral Stokes shift or solvation times. The final column of Table 1 lists estimates for the fraction of the Stokes shift observed using TCSPC.[17] With the exception of $[P_{14\,666}][Tf_2N]$ only about half of the solvation response is represented by these values of $\langle \tau_{solv} \rangle$. When comparing reaction and solvation times in the following section, we recognize the uncertainty caused by the missing fast components of solvation by plotting as the lower uncertainty limits of $\langle \tau_{solv} \rangle$ the values $(1 - f_{obs})\langle \tau_{solv} \rangle$.

A. Biphenyl Acridinium. Representative steady-state spectra of biphenyl acridinium ($BPAc^+$) in conventional solvents and in the ionic liquid $[Im_{21}][Tf_2N]$ are shown in Figure 2. In the weakly polar solvent tetrahydrofuran (THF), the S_1 absorption of $BPAc^+$ shows clear vibronic structure and the emission spectrum is approximately the mirror image of the absorption. Emission in THF is mainly from the LE state localized on the acridinium ring. In more polar solvents such as acetonitrile and in ionic liquids, the absorption spectrum broadens but does not shift appreciably and dual emission is observed. LE emission

Table 1. Selected Characteristics of the Ionic Liquids Studied[a]

ionic liquid	[IP]/(mol dm^{-3})	λ_{C153}/ (kJ mol^{-1})	ΔG_{C153}/ (kJ mol^{-1})	T/°C	η/cP	$\langle\tau_{solv}\rangle$/ns	f_{obs}
$[Im_{21}][Tf_2N]$	3.6[b]	13	43	25	35	0.14 ± 0.02	0.53
$[Im_{41}][BF_4]$	5.3[c]	13	45	10	267[e]	0.8 ± 0.2	0.50
$[Im_{41}][PF_6]$	4.8[c]	13[e]	46[e]	25	196[e]	1.0 ± 0.1[e,f]	0.65
				70	29[e]	0.14 ± 0.02[f]	0.45
$[N_{3111}][Tf_2N]$	3.8[d]	14	43	25	82	0.37 ± 0.07	0.46
				65	20	0.07 ± 0.01	0.58
$[N_{ip311}][Tf_2N]$	3.4[c]	13[e]	43[e]	10	264[e]	1.2 ± 0.2[g]	0.50
				25	113[e]	0.51 ± 0.08[e]	0.57
				65	23[e]	0.09 ± 0.03[e]	~0.4
$[Pr_{31}][Tf_2N]$	3.4[c]	13[e]	43[e]	25	54[e]	0.28 ± 0.04[e]	0.52
$[Pr_{41}][Tf_2N]$	3.3[c]	13[e]	42[e]	21	93[e]	0.46 ± 0.07	0.50
$[P_{14\,666}][T_2fN]$	1.4[b]	10[e]	43[e]	10	900	~18[g]	
				45	125	2.5 ± 0.3	1.0

[a] [IP] denotes the concentration of ion pairs (formula units), λ_{C153} (±1 kJ/mol) and ΔG_{C153} (±2 kJ/mol) are the solvent reorganization energy and free energy change associated with the $S_0 \leftrightarrow S_1$ transition of C153 [17] at 25 °C. η is the solvent viscosity (±10%) and $\langle\tau_{solv}\rangle$ the integral solvation time measured with C153 using TCSPC at the temperatures listed (eq 1). f_{obs} is the estimated fraction of the total solvation response observed with the ~25 ps resolution of the TCSPC experiment. Data are from refs 17, 89a, and 98−100, or from the present study. [b] Reference 98. [c] Reference 89a. [d] Reference 99. [e] Reference 17. [f] Reference 100. [g] Denotes a value estimated on the basis of data at other temperatures.

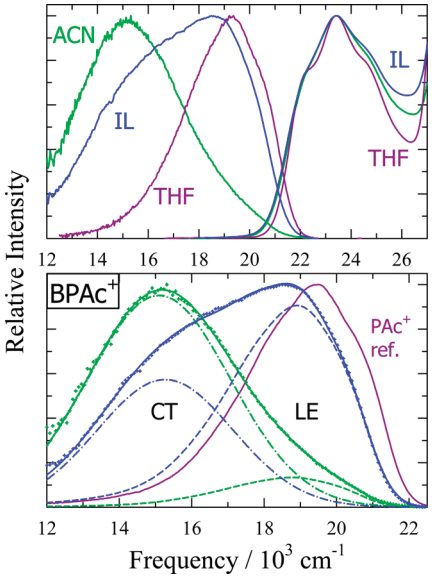

Figure 2. Top panel: Absorption and emission spectra of $BPAc^+$ in THF, ACN, and $[Im_{21}][Tf_2N]$ (IL). Bottom panel: Reference emission spectrum of PAc^+ in acetonitrile and fits of the emission of $BPAc^+$ in acetonitrile and $[Im_{21}][Tf_2N]$ showing decompositions into LE (dashed) and CT (dashed−dotted) components, as described in the text.

occurs at approximately the same frequency as in THF (~19 000 cm^{-1}), and a new emission band appears near 15 000 cm^{-1} attributed to a CT state reached by electron transfer from the biphenyl donor to the acridinium acceptor.[87]

To decompose steady-state and time-resolved emission into LE and CT contributions, we use the spectrum of the reference compound 9-phenyl-10-methylacridinium (bottom panel of Figure 2), which does not undergo charge transfer. Specifically, we assume that the line shape ($\chi(\nu) \propto F(\nu)/\nu^3$, where $F(\nu)$ is the emission spectrum) of the LE emission of $BPAc^+$ in a given solvent is a slightly broadened and shifted version of the line shape of PAc^+ in that solvent. We further assume that the CT emission line shape is Gaussian and thereby fit fluorescence spectra to the function

$$F(\nu) \propto \nu^3\{(1-f_{CT})\int \chi_{LE}(\nu-\delta)\, g_{LE}(\delta)\, d\delta + f_{CT}\chi_{CT}(\nu)\} \quad (2)$$

where

$$g_{LE}(\delta) = \frac{1}{\sqrt{2\pi\sigma_{LE}^2}} \exp\left\{-\frac{(\delta-\delta_{LE})^2}{2\sigma_{LE}^2}\right\} \quad (3)$$

$$\chi_{CT}(\nu) = \frac{1}{\sqrt{2\pi\sigma_{CT}^2}} \exp\left\{-\frac{(\nu-\nu_{CT})^2}{2\sigma_{CT}^2}\right\} \quad (4)$$

The parameter f_{CT} is the relative population of the CT state, which is of most interest for understanding the kinetics of the LE → CT reaction. The bottom panel of Figure 2 illustrates the LE (dashed) and CT (dashed−dotted) component spectra obtained from such fitting.

There are a total of five parameters in this model, δ_{LE}, Γ_{LE}, f_{CT}, ν_{CT}, and Γ_{CT}, where the $\Gamma_i = (8 \ln 2)^{1/2}\sigma_i$ are full widths. In many cases, especially the low-spectral resolution TCSPC data, the spectra do not uniquely determine all five parameters. A survey of steady-state spectra in high-polarity conventional solvents and ionic liquids shows the width parameters can be fixed at average values Γ_{LE} = 770 cm^{-1} and Γ_{CT} = 4300 cm^{-1} without degrading the quality of the fits significantly. From fits constrained in this way we find that the LE and CT frequencies in ionic liquids are only slightly red-shifted relative to those in high-polarity conventional solvents such as acetonitrile, dimethylformamide, and methanol. The frequency of the LE band is 200 ± 100 cm^{-1} and the CT band 650 ± 300 cm^{-1} lower in the case of ionic liquids, indicating that $BPAc^+$ feels an effective polarity just slightly higher than the polarities of these conventional solvents.

dx.doi.org/10.1021/jp200339e |J. Phys. Chem. B 2011, 115, 6592–6607

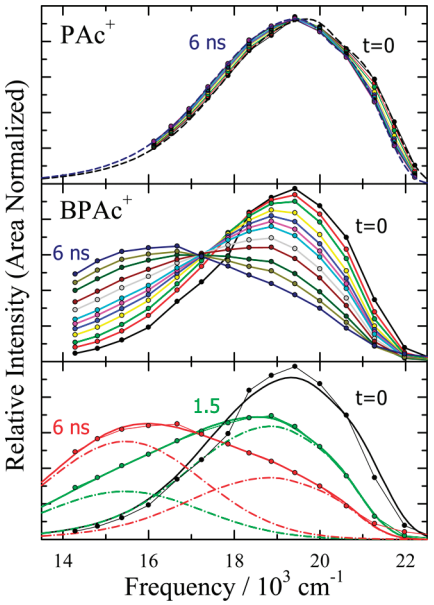

Figure 3. Time-resolved emission spectra of PAc^+ (top panel) and $BPAc^+$ in $[N_{ip311}][Tf_2N]$ at 25 °C. The points are reconstructed spectra at times of 0, 0.1, 0.2, 0.4, 0.6, 0.8, 1, 1.5, 2, 3, 4, and 6 ns. The dashed curves in the top panel and the thick curves in the bottom panel show representative fits and decompositions into LE (dashed) and CT (dashed−dotted) components.

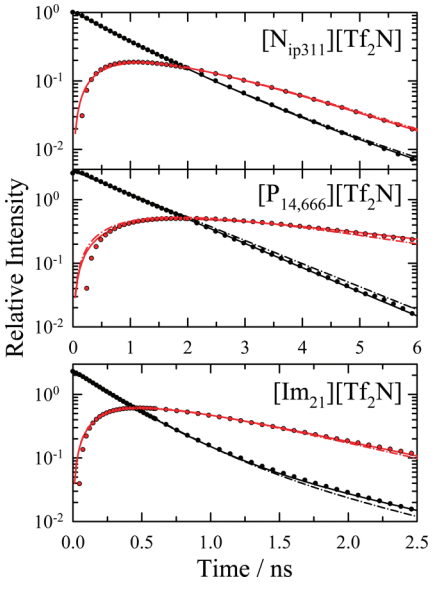

Figure 4. Representative decays of LE (black) and CT (red) band intensities in three ionic liquids. The $[P_{14\,666}][Tf_2N]$ data were recorded at 45 °C and the other two data sets at 25 °C. Points indicate observed relative intensities and the curves indicate unconstrained (solid) and constrained (dashed−dotted) fits to eqs 5−7 (r_{rad} = 0.55).

A much more obvious distinction between conventional solvents such as acetonitrile and ionic liquids illustrated by Figure 2 is the fact that the relative contribution of CT emission is much smaller in ionic liquids; f_{CT} = 0.48 ± 0.09 compared 0.89 ± 0.02 in high-polarity conventional solvents. This difference is a kinetic effect. In conventional solvents the LE ↔ CT reaction is much faster than S_1 depopulation so that, apart from a radiative rate factor,

Scheme 1

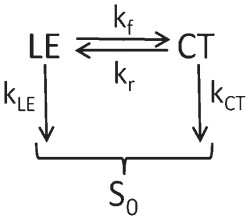

f_{CT} indicates the fractional population of the CT state in equilibrium.[58] In ionic liquids on the other hand, S_1 decay is competitive with charge transfer, which means that the steady-state spectra do not reflect equilibrium excited-state populations.

Representative time-resolved emission spectra of PAc^+ and $BPAc^+$ in the ionic liquid $[N_{ip311}][Tf_2N]$ are shown in Figure 3. As illustrated by the top panel, the LE-state surrogate PAc^+ undergoes a small (~200 cm^{-1}) dynamic Stokes shift in ionic liquids. In the cases we have examined, the Stokes shift times of PAc^+ are within uncertainties of those measured using the probe C153. We expect similar Stokes shifts of the LE band of $BPAc^+$, which means that emission decays measured at individual wavelengths will reflect both the LE ↔ CT interconversion and the solvation of the LE and possibly CT bands. For this reason we analyzed kinetics by fitting the time-resolved spectra as described above. Typical fits are shown in the bottom panel of Figure 3. In all cases we found that satisfactory fits to the time-evolving spectra could be obtained by constraining the CT band to have the same frequency observed in the steady-state spectrum (ν_{CT} ~ 14 700 cm^{-1}) and allowing the LE band position, as specified by δ_{LE}, to vary by a few hundred wavenumbers. From such fits we derived the time-dependent relative intensities of the LE and CT bands for kinetic analysis, free of the effect of Stokes shifting. Three examples of intensity decay data are shown in Figure 4. All of the intensity data generated in this manner could be well-represented by biexponential functions of time, and parameters obtained from unconstrained biexponential fits are listed in Table 2.

In conventional solvents, a two-state description of the LE → CT reaction was found to be appropriate[58], and we therefore analyzed band intensities using this kinetic model, which is defined in Scheme 1. Assuming that excitation occurs to only the LE state, the time-dependent band intensities are given by

$$I_{LE}(t)/I_{LE}(0) = \left(\frac{1}{\lambda_+ - \lambda_-}\right)\{(Y-\lambda_-)e^{-\lambda_- t} + (\lambda_+ - Y)e^{-\lambda_+ t}\} \quad (5)$$

$$I_{CT}(t)/I_{LE}(0) = \left(\frac{k_{rad}^{CT}}{k_{rad}^{LE}}\right)\frac{k_f}{(\lambda_+ - \lambda_-)}\{e^{-\lambda_- t} - e^{-\lambda_+ t}\} \quad (6)$$

where

$$\lambda_\pm = \frac{1}{2}\{(X+Y) \pm \sqrt{(X-Y)^2 + 4k_f k_r}\} \quad (7)$$

$X = k_{LE} + k_f$, $Y = k_{CT} + k_r$, and where k_{rad}^I is the radiative rate constant of state I. In comparing the measured intensities to this model, we fixed the rate constant k_{LE} to the intensity decay rates of PAc^+, which are listed in Table 2. The parameters k_f, k_{CT}, $K_{eq} = k_f/k_r$, and $r_{rad} = k_{rad}^{CT}/k_{rad}^{LE}$ were allowed to vary. Examples of

Table 2. Kinetic Parameters of the LE → CT Reaction of $BPAc^+$ in Various Ionic Liquids[a]

			biexponential fits[b]					two-state fits[c]				
ionic liquid	T /°C		a_1	τ_1	a_2	τ_2	$\langle\tau\rangle$	k_{LE}	k_{CT}	k_f	K_{eq}	τ_{rxn}[d]
$[Im_{21}][Tf_2N]$	25	LE	0.93	0.31	0.07	1.09	0.36	2.8	11.9	27.1	24	0.32 ± 0.07
		CT	−0.52	0.25	0.48	1.01						
$[Im_{41}][PF_6]$	25	LE	0.61	0.17	0.39	0.57	0.32	1.4	4.5	6.6	3.1	1.6 ± 0.4
		CT	−0.49	0.18	0.51	0.84						
$[Im_{41}][PF_6]$	70	LE	0.24	0.72	0.76	2.08	1.75	5.0	13.3	39.8	5.2	0.24 ± 0.07
		CT	−0.48	0.70	0.52	2.98						
$[N_{3111}][Tf_2N]$	25	LE	0.65	0.76	0.35	1.48	1.01	2[e]	6.6	10.2	6.3	1.0 ± 0.2
		CT	−0.50	0.50	0.50	1.97						
$[N_{3111}][Tf_2N]$	65	LE	0.87	0.20	0.13	0.77	0.27	5[e]	13.3	48.4	7.3	0.20 ± 0.07
		CT	−0.46	0.18	0.54	0.79						
$[N_{ip311}][Tf_2N]$	25	LE	0.80	0.87	0.20	1.76	1.05	1.9	7.5	8.1	16	1.1 ± 0.2
		CT	−0.51	0.69	0.49	1.77						
$[N_{ip311}][Tf_2N]$	65	LE	0.83	0.19	0.17	0.67	0.27	5.0	15.1	39.7	10	0.22 ± 0.05
		CT	0.51	0.17	0.49	0.81						
$[P_{14\,666}][Tf_2N]$	45	LE	1.00	1.13	—	—	1.13	3.1	3.4	5.3	>50	1.6 ± 0.2
		CT	−0.52	1.14	0.48	3.38						

[a] All times are in units of nanoseconds and rate constants in units of 10^8 s^{-1}. [b] Parameters of unconstrained fits of LE and CT band intensities to $I(t)/I(0) = a_1 \exp(-t/\tau_1) + a_2 \exp(-t/\tau_2)$. $\langle\tau\rangle$ is the average decay time, $a_1\tau_1 + a_2\tau_2$. [c] Parameters of fits to eqs 5−7 with $r_{rad} = 0.55$. Values of k_A are fixed at the values $k_A = 1/\tau_{PAc}$, where τ_{PAc} is the lifetime observed for PAc^+. [d] τ_{rxn} is the best estimate of the reaction time constant (see text). [e] Values assumed to be the same as those of $[N_{ip311}][Tf_2N]$.

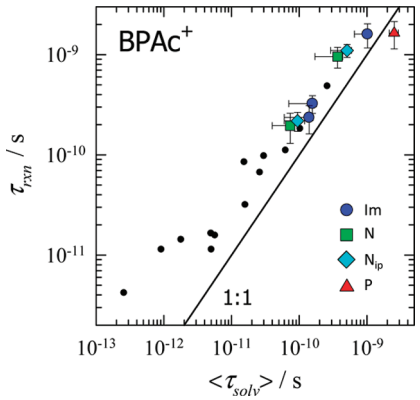

Figure 5. Time constants τ_{rxn} of the LE → CT reaction of $BPAc^+$ in conventional solvents (small symbols from ref 58) and ionic liquids (large colored symbols) plotted versus integral solvation times $\langle\tau_{solv}\rangle$ (eq 1) measured with C153.

such fits are shown in Figure 4 and parameters derived from them listed in Table 2. As illustrated in Figure 4, the kinetics of the LE and CT band intensities are reasonably represented by this two-state description. On the basis of quantum yield data in conventional high-polarity solvents, a value of $r_{rad} = k_{rad}^{CT}/k_{rad}^{LE} \sim 0.3$ is expected for $BPAc^+$. Somewhat larger values are obtained when this parameter is allowed to vary freely (solid curves in Figure 4). The parameters in Table 2 are those derived using an average value of $r_{rad} = 0.55$ (dashed−dotted curves) which fit the ionic liquid data much better than does $r_{rad} = 0.3$. The values of K_{eq} obtained using either choice of r_{rad} are typically much larger than unity as expected on the basis of values observed in high-polarity conventional solvents. The variation in K_{eq} among the different ionic liquids does not appear to be sensibly related to their relative polarities, and these variations probably only reflect uncertainties in the data. As a final measure of the time constant for the LE → CT reaction, τ_{rxn}, which is listed in the final column of Table 2, we use the average of the times (k_f^{-1}) determined from the k_f values obtained from unconstrained fits and from fits in which $r_{rad} = 0.3$ is used. The difference between the two k_f^{-1} values provides an estimate of the uncertainty in τ_{rxn}.

Figure 5 compares the times for the LE → CT reaction of $BPAc^+$ to average solvation times measured using the C153 probe. Data in both conventional polar solvents (small circles from ref 58) and ionic liquids (large symbols) are shown. With the possible exception of $[P_{14\,666}][Tf_2N]$, the reaction times in ionic liquids appear to follow the same correlation with solvation times observed in conventional solvents. The ionic liquid data overlap the data in the long-chain alcohols *n*-pentanol and *n*-decanol, which have the slowest solvation times (100 and 260 ps[54]). Thus, with respect to its effect on charge transfer in $BPAc^+$, there appears to be nothing distinctive about the environment presented by most of the ionic liquids studied beyond the fact that solvation is slow. As already discussed, the energetics of reaction are likely to be somewhat different in the case of $[P_{14\,666}][Tf_2N]$ (Table 1), which could be the reason for its lack of correlation with the remaining data. Alternatively, we note that the heterogeneous structure created by the high alkyl content of the $P_{14\,666}^+$ cation[92] appears to markedly influence the solvation times of C153.[17] In this solvent, the reaction time of $BPAc^+$ is comparable to the times observed in other ionic liquids of comparable viscosity, but the solvation time is roughly 5-fold slower.[17] This latter effect could also account for the deviation $[P_{14\,666}][Tf_2N]$ displays compared to the other ionic liquid data.

It should be noted that these and the corresponding kinetic data in CVL and bianthryl are not recorded under isothermal conditions. We instead often have used one or more temperatures near 25 °C in order to optimize conditions for observing a reaction or to provide more than one rate in a given solvent. We

dx.doi.org/10.1021/jp200339e |J. Phys. Chem. B 2011, 115, 6592–6607

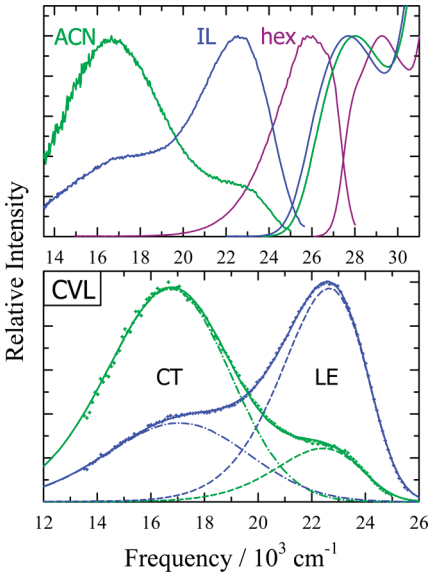

Figure 6. Top panel: Steady-state absorption and emission spectra of CVL in *n*-hexane (hex), ACN, and $[N_{3111}][Tf_2N]$ (IL). Bottom panel: Decomposition of the acetonitrile and $[N_{3111}][Tf_2N]$ spectra into LE (dashed) and CT (dashed−dotted) components as described in the text.

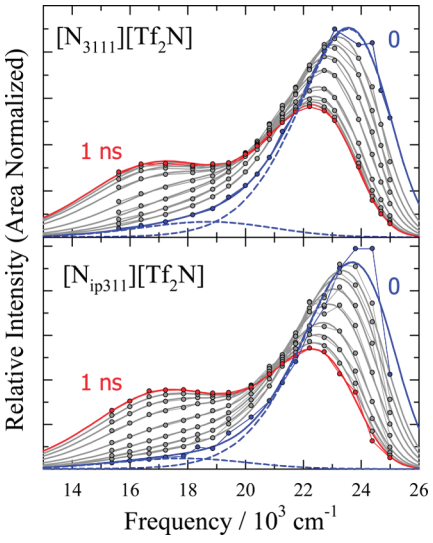

Figure 7. Time-resolved emission spectra of CVL in two ionic liquids. The connected points are the reconstructed spectra and the heavy smooth curves are fits to these data as described in the text. Times shown are 0, 25, 50, 100, 200, 400, 600, 800, and 1000 ps. The blue dashed lines show the LE and CT components at $t = 0$.

do so under the assumption that all three reactions, at least in high-polarity solvents such as ionic liquids, involve low or negligible (≤5 kJ/mol) intrinsic barriers to reaction. In this case, the dominant effect of temperature is to change solvation times because, like viscosities, these times exhibit activation energies of 30−40 kJ/mol.[89b]

B. Crystal Violet Lactone. Steady-state spectra of CVL are shown in Figure 6. In contrast to $BPAc^+$ (and BA) the frequency of the $S_0 \rightarrow S_1$ (LE) absorption of CVL varies significantly with solvent polarity. The 1200−1400 cm^{-1} red shifts observed between the absorption in *n*-hexane and high-polarity solvents

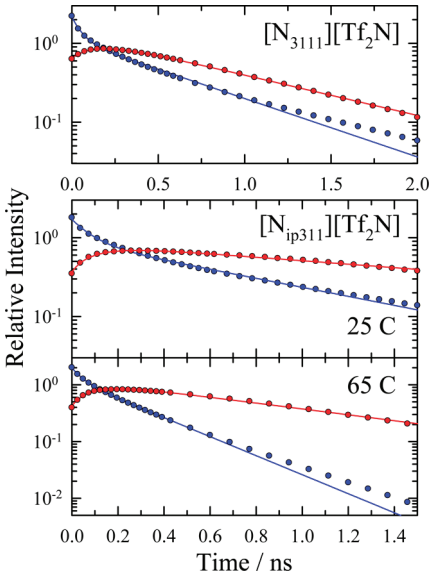

Figure 8. Time dependence of the LE (blue) and CT (red) band intensities obtained from fits of CVL emission spectra. Points are the intensity data, and curves are unconstrained biexponential fits to these data.

such as acetonitrile indicate that the LE state of CVL is substantially more polar than the ground state. For this reason the LE emission of CVL depends much more on solvent polarity than in the case of the other two solutes studied. As in $BPAc^+$, both the LE and CT bands contribute to the emission in solvents of moderate to high polarity, and in CVL these peaks are typically better separated than in $BPAc^+$. To determine characteristics of the LE and CT emission bands, we employ the same procedure for fitting the spectra as described for $BPAc^+$. The only difference is that the emission of CVL in *n*-hexane, where the CT contribution is assumed negligible, is used to obtain the LE line shape. Representative decompositions into LE and CT components are shown in the bottom panel of Figure 6. Once again, the much larger contribution of CT emission in the spectrum of acetonitrile compared to that in $[N_{3111}][Tf_2N]$ is due to the fact that emission of CVL is not equilibrated in ionic liquids, whereas it is in most conventional solvents.[62]

Examples of time-resolved emission spectra of CVL in ionic liquids are provided in Figure 7. The features of these spectra are similar to those observed in the $BPAc^+$ reaction, but in CVL the difference in polarity between the S_0 and LE states leads to a much larger (~2000 cm^{-1}) dynamic Stokes shift of the LE band occurring simultaneously with the LE → CT reaction. This Stokes shift tends to blur any isoemissive points in the area-normalized spectra,[93] but the two-state character of the spectral dynamics is still evident. As in the case of $BPAc^+$, we fit the time-resolved spectra (eqs 2−4) in order to obtain information about the reaction kinetics free from contamination by this spectral shifting. To within uncertainties, the reconstructed spectra (points in Figure 7) could be fit by constraining the width parameters Γ_{LE} (~1900 cm^{-1}) and Γ_{CT} (~5000 cm^{-1}) as well as the frequency of the CT emission ($\nu_{CT} \cong$ 17 000 cm^{-1}) to values obtained from steady-state spectra and only allowing δ_{LE} and f_{CT} to vary with time. The smooth curves in Figure 7 are the results of such fits.

Representative LE and CT band intensities derived from this analysis are shown in Figure 8. These intensities are not as cleanly

Table 3. Parameters Characterizing the Emission Dynamics of CVL[a]

			biexponential fits[b]				time estimates[c]			
IL	T/°C		a_1	τ_1	a_2	τ_2	τ_{fast}	$\langle\tau_{LE}\rangle$	k_f^{-1}	τ_{rxn}[d]
$[Im_{21}][Tf_2N]$	25	LE	0.42	0.043	0.58	0.24	0.059	0.17	0.091	0.10 ± 0.05
		CT	−0.40	0.11	0.60	0.34				
$[N_{3111}][Tf_2N]$	25	LE	0.49	0.055	0.51	0.59	0.076	0.35	0.12	0.18 ± 0.13
		CT	−0.33	0.15	0.67	0.85				
$[N_{ip311}][Tf_2N]$	25	LE	0.49	0.082	0.51	0.76	0.10	0.48	0.21	0.26 ± 0.19
		CT	−0.36	0.12	0.64	2.0				
$[N_{ip311}][Tf_2N]$	65	LE	0.38	0.044	0.62	0.26	0.068	0.18	0.14	0.13 ± 0.06
		CT	−0.40	0.11	0.60	0.84				
$[Pr_{31}][Tf_2N]$	25	LE	0.40	0.059	0.60	0.51	0.087	0.35	0.059	0.17 ± 0.15
		CT	−0.40	0.12	0.60	1.4				
$[P_{14\,666}][Tf_2N]$	45	LE	0.22	0.67	0.78	5.9	1.1	4.9	5.3	3.7 ± 2.0
		CT	0.49	1.3	0.51	10.0				

[a] All times are in units of nanoseconds. [b] Parameters of unconstrained fits of LE and CT band intensities to $I(t)/I(0) = a_1 \exp(-t/\tau_1) + a_2 \exp(-t/\tau_2)$. [c] Three possible measures of reaction time: $\langle\tau_{fast}\rangle$ is the average short component of the LE decay and CT rise, $\langle\tau_{LE}\rangle$ is the integral decay time of the LE band, and k_f^{-1} is the inverse of the forward rate constant obtained from unconstrained fits to the two-state model described by eqs 5−7. [d] Best estimate of reaction rate obtained from the average of the previous time estimates and uncertainties given by half of the spread of these values.

represented by the simple kinetic model applied to the $BPAc^+$ data. For one thing, the CVL band intensities are not as well-represented by biexponential functions of time. As can be seen from Figure 8, although biexponential fits (smooth curves) provide reasonable characterizations of the data (points), the fit is not as accurate as in the $BPAc^+$ case. Because the quantum yield of CVL emission is low ($<10^{-2}$ in highly polar solvents[61] and even lower in some ionic liquids[51]), it seems reasonable to ascribe the lack of perfect biexponential fits to impurity fluorescence from the ionic liquid solvents that is not completely removed by solvent subtraction. A more serious departure from simple two-state kinetics is that, with the exception of $[P_{14\,666}][Tf_2N]$, the reconstructed spectra show significant CT intensity ($f_{CT} \sim 0.2$) at the earliest times. (See Figure 7.) This prompt CT emission might also result from residual impurity emission or from fast components of the reaction not adequately captured in the present experiments.[62] Whatever the source, the presence of this prompt CT emission means that the CVL data cannot be fit accurately using eqs 4−6. For this reason we can only make rough estimates of the times associated with the LE → CT reaction. We do so using the data summarized in Table 3. The columns labeled "biexponential fits" are the parameters obtained from independent fits of the LE and CT intensities. From these fits, as well as from constrained fits in which the CT intensity is required to be zero at $t = 0$, we obtain average values of the fast time constant associated with decay of LE and the rise of CT intensity, labeled τ_{fast}. This time should provide an approximate lower limit for the reaction time. The integral decay time of the LE intensity, $\langle\tau_{LE}\rangle$, is an approximate upper limit for the reaction time. This measure would be appropriate if the reaction was irreversible and nonexponential. Finally, the inverse of the forward reaction rate constant obtained from the best simultaneous fit of the LE and CT intensities to eqs 5−7, k_f^{-1}, provides a third estimate of the reaction time. As a practical, albeit crude, measure of the LE → CT reaction time, we take the average of these three estimates and, as a measure of uncertainty, use the spread in these times.

These reaction times are compared to solvation times of C153 in Figure 9. Also shown are reaction times observed in high-polarity

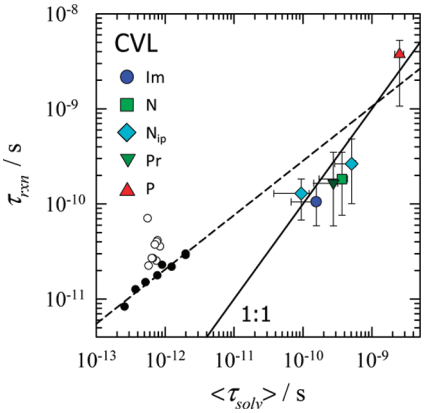

Figure 9. Time constants of the LE → CT reaction of CVL in conventional solvents at 25 °C (small symbols) from ref 62 and ionic liquids (large colored symbols) plotted versus integral solvation times $\langle\tau_{solv}\rangle$ measured with C153. Among the conventional solvents, open symbols indicate low to moderate polarity and filled symbols high-polarity solvents ($\varepsilon > 25$). The dashed line is a fit to the latter data.

conventional solvents (small filled circles), where determination of the reaction time is straightforward.[62] In the ionic liquids studied, the estimated reaction times are within a factor of 2 of the integral solvation times, with most reaction times being somewhat less than solvation times. In contrast, in conventional solvents of low viscosity, reaction times are considerably greater than solvation times. But an extrapolation of the relationship between τ_{rxn} and $\langle\tau_{solv}\rangle$ in high-polarity conventional solvents to the regime found in ionic liquids (dashed line, $\tau_{rxn} \propto \langle\tau_{solv}\rangle^{0.6}$) suggests that the behavior in ionic liquids might not be qualitatively different from that in conventional solvents. (Note that we consider only strongly polar solvents in this comparison because the data in other solvents (open symbols) suggest solvent polarity also has a strong effect on reaction rates.[62]) Unfortunately, unlike the other two reactions studied here, side reactions[61] prevent measurement of the charge transfer of CVL in *n*-alcohol solvents in order to extend the conventional solvent

dx.doi.org/10.1021/jp200339e |*J. Phys. Chem. B* 2011, 115, 6592–6607

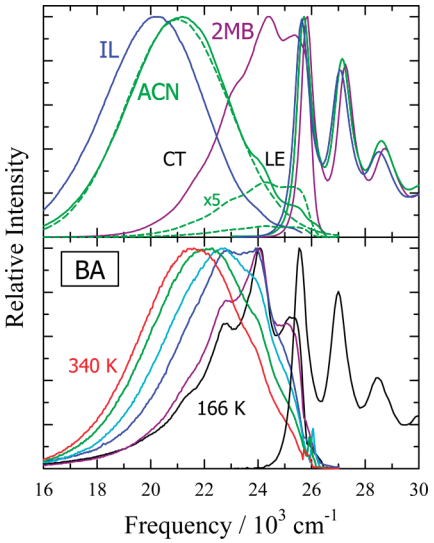

Figure 10. Steady-state spectra of bianthryl. Top panel: Absorption and emission spectra of BA in 2-methylbutane (2MB), ACN, and $[Im_{21}][Tf_2N]$ (IL) at 25 °C (in order of decreasing frequency). Dashed green curves show an approximate decomposition of the acetonitrile spectrum into LE and CT components. Bottom panel: Room-temperature absorption and temperature-dependent emission spectra of BA in $[P_{14\,666}][Tf_2N]$. The temperatures shown are 166, 204, 222, 260, 281, and 340 K in order of decreasing frequency. (Note that the highest energy peak in the LE emission at low temperature is distorted by the inner filter caused by a high OD (0.35) of this sample.)

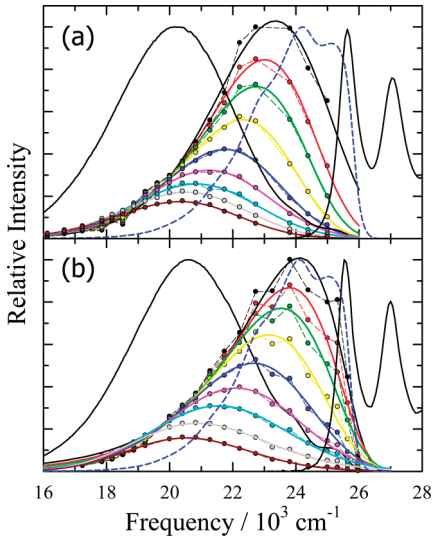

Figure 11. Time-resolved emission spectra (connected points) of bianthryl in (a) $[Im_{21}][Tf_2N]$ at 25 °C and (b) $[Pr_{41}][Tf_2N]$ at 21 °C and fits of these data to log-normal line shape functions (smooth curves). Spectra in panel a are at times of 0, 10, 20, 40, 80, 160, 320, 640, and 4000 ps and in b at 0, 20, 40, 80, 160, 320, 640, 2000, and 10 000 ps. Also shown (black curves) are absorption and steady-state emission spectra and estimated time-zero spectra (dashed blue curves).

data to the ionic liquid regime. Thus, the most that can be concluded is that the CVL reaction is probably controlled by solvation dynamics in both high-polarity conventional solvents and ionic liquids. Additional experiments would be needed to more clearly establish whether the nature of this solvent control is the same in these two solvent classes.

C. Bianthryl. Steady-state spectra of bianthryl are shown in Figure 10. The room-temperature spectra in the top panel illustrate the relative solvent insensitivity of the anthracene-like absorption spectrum of bianthryl. This weak solvatochromism indicates that the S_0 and LE states of bianthryl have similar polarities. The emission of bianthryl is structured in nonpolar solvents like 2-methylbutane and is characteristic of the LE state. In highly polar solvents such as acetonitrile and ionic liquids, the broad, red-shifted emission of the CT state dominates the spectrum, with the only indication of some LE population being the residual structure on the blue side of the emission band. In contrast to the previous two cases, the CT emission of bianthryl accounts for a larger proportion of the emission and it is red-shifted in the ionic liquid $[Im_{21}][Tf_2N]$ compared to acetonitrile. The reason for this distinction is that the S_1 lifetime of bianthryl (20−30 ns) is sufficiently large that the steady-state emission now does reflect equilibrium between the LE and CT states. The greater CT fraction and red shift indicate that bianthryl senses a more polar environment in $[Im_{21}][Tf_2N]$ than it does in acetonitrile.

The bottom panel of Figure 10 shows the temperature dependence of the steady-state emission spectra of bianthryl in $[P_{14\,666}][Tf_2N]$. This ionic liquid readily forms a glass upon cooling (T_g = 197 K [94]), which allows easy access to a rigid solvent environment. Under such conditions, exemplified by the 166 K data in Figure 10, the LE → CT reaction is inhibited and only the structured emission of the LE state is observed. CT emission becomes evident above the glass transition, even at temperatures as low as 220 K where extrapolated viscosities exceed 10^6 cP. At room temperature, where reaction equilibrium is expected, CT emission accounts for about 75% of the spectrum. Both the smaller CT fraction and the lower frequency of the CT emission indicate that bianthryl sees $[P_{14\,666}][Tf_2N]$ as substantially less polar than $[Im_{21}][Tf_2N]$ or the other ionic liquids studied here.

Time-resolved spectra of bianthryl in two ionic liquids are provided in Figure 11. These spectra do not display clear signatures of a two-state reaction as did the spectra of $BPAc^+$ and CVL. To within the temporal and spectral resolution employed here, it is difficult to discern any genuine structure in the time-resolved spectra or approximate isoemissive points in area-normalized spectra as were present in Figures 3 and 6. Instead, as shown in Figure 11, the reconstructed spectra are reasonably represented by single log-normal line shape functions. In this sense, the time-dependent spectra of bianthryl resemble those of a nonreactive probe such as C153 whose emission shifts in time due to solvation dynamics. The lack of obvious dual emission and resemblance to the dynamics observed for a pure solvation process result from the fact that the LE → CT reaction in bianthryl entails essentially barrierless motion along an adiabatic reaction coordinate comprised mainly of solvent polarization modes. The existence of a change of electronic state is nevertheless clearly signaled by the large drop in intensity as the spectrum shifts. In nonpolar solvents, where the LE state is primarily responsible for emission, the radiative rate of bianthryl is $\sim 10^8$ s^{-1}, whereas in highly polar solvents such as acetonitrile, where most emission is from the CT state, k_{rad} is about 10-fold smaller.[80] The loss of intensity in the time-dependent emission therefore reports on the evolution from the LE-like Franck−Condon state to a CT-like state at long times, and we will use this intensity change to measure reaction times.

The dashed curves in Figure 11 show the time-zero spectra[95] predicted for the LE state immediately after excitation. Although the peak frequency and perhaps even the structure in the earliest measured spectrum of bianthryl in $[Pr_{41}][Tf_2N]$ are similar to

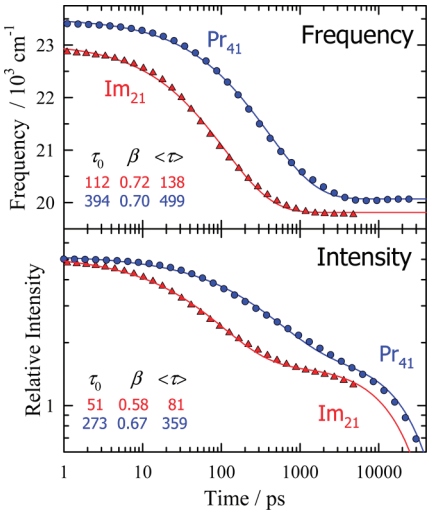

Figure 12. Characteristics of bianthryl emission obtained from log-normal fits of the (ν^3 normalized) time-evolving spectra in Figure 11. The top panel shows the peak frequencies and the bottom panel integral intensities in $[Im_{21}][Tf_2N]$ at 25 °C (red triangles) and $[Pr_{41}][Tf_2N]$ at 21 °C (blue circles). The smooth curves are fits to these data according to eqs 8 and 9, and the inset tables provide selected parameters from these fits.

Table 4. Parameters Characterizing the Emission Dynamics of Bianthryl[a]

		frequency shift[b]		intensity decay[c]			
ionic liquid	T/°C	$\Delta\nu$	$\tau_{\Delta\nu}$	τ_{dec}	τ_{II}	$\tau_{\leq 420}$	τ_{rxn}[d]
$[Im_{21}][Tf_2N]$	25	3.1	0.17 ± 0.04	26.1	0.076	0.046	0.06 ± 0.03
$[Im_{41}][BF_4]$	10	2.9	0.9 ± 0.2	31.3	0.41	0.45	0.43 ± 0.09
$[N_{3111}][Tf_2N]$	25	3.4	0.39 ± 0.08	30.8	0.17	0.32	0.25 ± 0.12
$[N_{ip311}][Tf_2N]$	10	3.4	1.3 ± 0.3	36.2	0.65	0.51	0.58 ± 0.12
	25	2.7	0.53 ± 0.11	35.6	0.33	0.29	0.31 ± 0.06
	65	3.0	0.16 ± 0.09	31.2	0.16	0.19	0.18 ± 0.04
$[Pr_{41}][Tf_2N]$	21	3.2	0.7 ± 0.2	35.7	0.41	0.57	0.49 ± 0.11
$[P_{14,666}][Tf_2N]$	10			32.7	4.8	2.6	4 ± 2
	45	3.3	4 ± 1	31.8	2.1	1.1	1.6 ± 1.0

[a] $\Delta\nu$ is in units of 10^3 cm^{-1} and all times in units of nanoseconds. [b] Stokes shift parameters obtained from log-normal fits of the time-resolved emission spectra to eq 8. The values listed are 2:1 weighted averages obtained from peak and first moment measures of frequency. [c] Intensity decay parameters: τ_{dec} is the longest component of the emission decays, τ_{II} is the integrated intensity decay time (eq 9) as described in the text, and $\tau_{\leq 420}$ is the average decay time obtained from fitting individual wavelengths on the blue edge of the spectrum (eq 10 and text). [d] τ_{rxn} is the best estimate for the reaction time obtained as the average of τ_{II} and $\tau_{\leq 420}$.

those in the predicted LE spectrum, upconversion experiments discussed later indicate that a substantial loss of intensity in the LE region occurs too rapidly to be measured in these TCSPC experiments. This observation is consistent with the fact that roughly half of the solvation dynamics in $[Pr_{41}][Tf_2N]$ and most of the other ionic liquids studied are missed by such experiments.[17,20,96] (See f_{obs} in Table 1.) The fact that we only observe the later portions of both solvation and reaction in bianthryl should be kept in mind when viewing the data obtained from such spectra.

Figure 12 illustrates the time dependence of the integrated intensities as well as the peak frequencies derived from log-normal

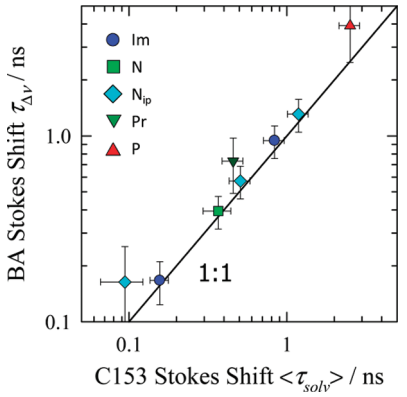

Figure 13. Comparison of the integral times associated with the Stokes shifts of C153 and bianthryl.

fits of the spectra in Figure 11. (Prior to analysis, the emission spectra were divided by ν^3 to remove the intensity effect caused by the dependence of radiative rate upon frequency, but similar results are also obtained using the emission spectra directly.) Both the frequency shifts and intensity decays of bianthryl in ionic liquids are highly nonexponential.

We first consider the frequency shifts. The dynamic Stokes shifts observed here for bianthryl are similar to those of C153 in ionic liquids. Using the ~25 ps time resolution afforded by TCSPC, the frequencies of both C153[17] and bianthryl can be fit to within uncertainties using a stretched exponential time dependence,

$$\nu(t) = \nu(\infty) + \Delta\nu \exp\{-(t/\tau_0)^{\beta}\} \quad (8)$$

The solid curves in the top panel of Figure 12 are fits to this functional form, with some fit parameters provided. Table 4 summarizes the magnitudes $\Delta\nu$ and the integral times $\tau_{\Delta\nu}$, calculated as $\tau_{\Delta\nu} = (\tau_0/\beta)\Gamma(1/\beta)$, for all of the systems studied. (Γ in this expression is the Γ function.) The magnitudes of the observed Stokes shifts of bianthryl are all near 3000 cm^{-1}, much larger than the shifts measured with C153, due to the larger polarity change in bianthryl. The values of β typically fall within the range of 0.6−0.7, similar to what was previously reported for C153 in a wide variety of ionic liquids.[17] Finally, as illustrated in Figure 13, the integral Stokes shift times measured with bianthryl ($\tau_{\Delta\nu}$) and C153 ($\langle\tau_{solv}\rangle$) are also nearly equal. In all cases the bianthryl shifts are slightly slower than those of C153 but in most cases the differences are within the anticipated uncertainties of the data. Thus, it seems clear that the Stokes shift dynamics of bianthryl faithfully reflect at least the slower portions of the solvation response measurable with the present experiments. Previous studies have come to this same conclusion and have provided Stokes shift times of bianthryl in several imidazolium ionic liquids.[45−47] In the two cases that overlap with the present data, the agreement with the integral times reported here is relatively poor. Detailed comparisons and discussion of the discrepancy are provided in the Supporting Information. Here we simply remark that we believe the $\tau_{\Delta\nu}$ (and the intensity decay times discussed next) reported in Table 4 are accurate to within their stated uncertainties for the particular time resolution employed. Both times represent only upper bounds to what would be observed with perfect time resolution, as do the solvation times of C153 used for comparison

To estimate reaction times, we make use of the conclusions of Barbara and co-workers based on detailed modeling of the

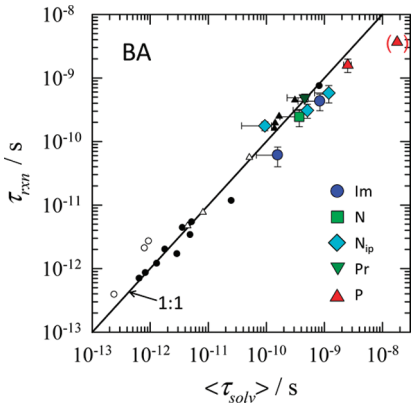

Figure 14. Estimated charge-transfer times of bianthryl versus integral solvation times measured with C153. Large symbols indicate data in ionic liquids. Small symbols indicate data in conventional solvents from refs 71 and 72 (filled symbols) and 82 (open symbols). Dipolar aprotic solvents are shown as small circles and *n*-alcohols as small triangles.

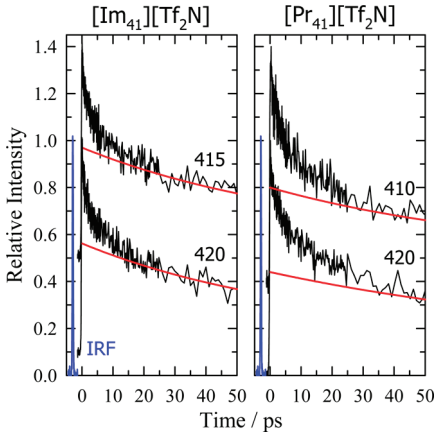

Figure 15. Comparison of normalized decays on the blue edge of the emission of bianthryl in $[Im_{41}][Tf_2N]$ and $[Pr_{41}][Tf_2N]$ at 21 °C recorded using TCSPC (smooth red curves) and fluorescence upconversion (noisy curves). The blue curves labeled IRF show the response function of the upconversion data (fwhm = 320 fs). Upconversion data are shown normalized to unit height. (The peak counts in these data sets were in the range of 100−300.) The TCSPC curves are multiexponential fits to the data. The 415 and 410 nm data have been shifted upward by adding 0.4 for clarity.

time-evolving emission spectra of bianthryl in several solvents.[72,73] They found that the progress of the LE → CT reaction, which they equated with the survival probability of the LE-state content in the mixed LE/CT wave function, can be tracked by monitoring either the integrated emission intensity or the intensity decays observed at wavelengths on the blue edge of the emission spectrum ($\lambda < 420$ nm) where CT contributions are small. We employ both intensity measures to estimate reaction times here. Examples of total intensity decay data are shown in the bottom panel of Figure 12. Such data were characterized by fitting to the function

$$I_{tot.}(t)/I_{tot.}(0) = f_{str}\exp\{-(t/\tau_0)^{\beta}\} + (1-f_{str})\exp(-t/\tau_{dec}) \quad (9)$$

The parameter τ_{dec} is the decay time of the equilibrated S_1 population, which is well-separated from other time constants of the emission decays. Example fits are the continuous curves shown in Figure 12 and selected parameters are listed in the inset table. For the ionic liquids studied values of f_{str} and β fall in the range of 0.7 ± 0.1 and 0.6 ± 0.1. Values of τ_{dec} and the integral intensity decay time, $\tau_{II} = (\tau_0/\beta)\Gamma(1/\beta)$, used as one measure of the reaction time, are compiled in Table 4. As an alternative measure of reaction time, we also determined the average of the decay times measured at individual wavelengths between 390 and 420 nm. Decay data were fit to a multiexponential form

$$I_\lambda(t)/I_\lambda(0) = \sum_{i=1}^{n} a_i \exp(-t/\tau_i) + a_{dec}\exp(-t/\tau_{dec}) \quad (10)$$

with n typically between 2 and 3 and the decay time determined from $\langle\tau_\lambda\rangle \geq \Sigma_i a_i\tau_i/\Sigma_i a_i$. The averages of $\langle\tau_\lambda\rangle$ over wavelengths $\lambda \leq 420$ nm are listed as $\tau_{\leq 420}$ in Table 4. As seen in this table, the two measures of reaction time, τ_{II} and $\tau_{\leq 420}$, agree only to about 33% on average. As a final estimate of reaction times, τ_{rxn}, we therefore take the mean of these two values and use their difference to estimate uncertainties.

Reaction times are plotted versus C153 solvation times in Figure 14. Included in this figure are data in conventional solvents (small symbols) from the early measurements of Barbara and co-workers[71,72] as well as the more recent data of Kovalenko et al.[82] Although most of the ionic liquid data fall slightly below the 1:1 line, there is no obvious distinction between the ionic liquid and conventional solvent data. As in the case of $BPAc^+$, it seems clear that the same relationship between charge transfer and solvation dynamics holds in both dipolar and ionic environments.

This result requires further discussion as it contradicts the conclusion reached by the two other groups who have recently studied bianthryl in ionic liquids. As described in the Introduction, both Nagasawa and co-workers[45,46] and Khara et al.[47] concluded that, in contrast to the case in conventional dipolar solvents, charge transfer in bianthryl occurs much more rapidly than solvation. The primary evidence for this contrary perspective came from femtosecond transient absorption (TA) data in the visible region by the Nagasawa group.[45] Nagasawa et al. measured integral rise times of an excited-state absorption attributed to the CT state to be in the range of 53−100 ps in the three imidazolium ionic liquids, $[Im_{41}][Tf_2N]$, $[Im_{41}][BF_4]$, and $[Im_{41}][PF_6]$, whereas they measured integral Stokes shift times of the emission ($\tau_{\Delta\nu}$) using TCSPC to be in the range of 650−2400 ps. In addition, Nagasawa et al. found that 30−50% of the rise of the CT transient absorption band occurs with an ultrafast time constant of 0.4−0.5 ps. Superficially, this comparison suggests that the charge-transfer reaction is at least an order of magnitude faster than solvation in these ionic liquids. But it is difficult to directly compare the results of experiments with such different time resolution: 200 fs in the TA experiments versus 30 ps in the TCSPC experiments. As already mentioned, TCSPC experiments only capture the longer time components of the dynamics and it is clear that Stokes shift components as fast as 0.5 ps would not be registered by this technique. Conversely, it may be that the lower sensitivity of the TA technique causes it to miss some of the small, long-time components detected in the TCSPC data.

Ideally, one would measure both the BA reaction dynamics and the solvation response with a technique that accurately captures both phenomena over the entire time range of relevance. We have not yet done so, but preliminary fluorescence upconversion data in $[Im_{41}][Tf_2N]$ and $[Pr_{41}][Tf_2N]$ provide some perspective on the TA results of Nagaswa et al.[45] Figure 15

shows a comparison of the decays measured on the blue edge of the emission spectrum, recorded using fluorescence upconversion with ~300 fs time resolution (noisy data) and using TCSPC (smooth fit curves). The decays at the two wavelengths shown are very similar. Multiexponential fits to the upconversion transients (to 500 ps) yield fast time constants of 3 ps (39%) and 55 ps (42%) in $[Im_{41}][Tf_2N]$ and 6 ps (44%) and 90 ps (40%) in $[Pr_{41}][Tf_2N]$. We do not detect any prominent subpicosecond components in these emission data. The fastest times we observe are similar to the intermediate CT rise components reported by Nagasawa et al.,[45] which ranged between 7 and 14 ps. The origins of the prominent sub-picosecond component present in the TA data but absent in emission experiments is unclear. But the data in Figure 15 suggest that by using TCSPC to examine this reaction, we are missing approximately 50% of the intensity decay used to monitor reaction progress. As indicated in Table 1 about 50% of the solvation response measured with C153 is also missed in TCSPC experiments. This comparison helps justify the use of TCSPC data to explore the connection between charge transfer and solvation in the bianthryl system, despite the fact that a large portion of the reaction is faster than can be detected.

4. SUMMARY AND CONCLUSIONS

In this study we have used time-correlated single-photon counting to measure the rates of three excited-state intramolecular electron-transfer reactions in an assortment of room-temperature ionic liquids. The solutes $BPAc^+$, CVL, and bianthryl were chosen because their excited-state reactions had already been characterized as being solvent controlled in conventional solvents. The goal here was to determine whether the same relationship between solvation and reaction previously established in dipolar solvents also holds in ionic liquids.

The simplest behavior was observed in the $BPAc^+$ reaction. In this case, emission from the LE state undergoes only a small dynamic Stokes shift, and time-evolving spectra closely resemble those expected for two-state kinetics between the LE and CT states. The lifetime of $BPAc^+$ is also sufficiently long (1−3 ns at 25 °C) that the reaction could be followed to equilibrium, and relatively accurate values of the LE → CT rate constant k_f obtained. With the exception of $[P_{14\,666}][Tf_2N]$, reaction times $\tau_{rxn} = k_f^{-1}$ were found to be strongly correlated to solvation times $\langle\tau_{solv}\rangle$ measured using the C153. The same correlation pertains to both ionic and dipolar solvents.

The situation is less straightforward in the case of the CVL reaction. Although the time-resolved spectra are clearly those of a two-state process, the integrated intensities of the LE and CT bands do not conform to a two-state kinetic scheme. It could be that heterogeneity of the ionic liquid environment leads to distributed kinetics in the CVL reaction,[66] thereby complicating the kinetics. But this seemingly more complex kinetics compared to $BPAc^+$ could also be caused by solvent emission, impossible to eliminate ionic liquids, contaminating the weak emission of CVL. Whatever the origin, the departures from a two-state kinetic scheme meant that reaction times could be only roughly estimated for the CVL reaction. To within the considerable uncertainties in the times deduced, an approximate equality $\tau_{rxn} \cong \langle\tau_{solv}\rangle$ was found between reaction and solvation times. An approximate equality of this sort was also noted by Samanta and co-workers in their recent study of CVL in ionic liquids.[51] This relationship apparently differs from what is observed in high-polarity dipolar solvents of low viscosity, where reaction is much faster than solvation. Whether this difference represents a qualitative distinction between the behavior in dipolar and ionic solvents cannot be determined with confidence from the present data. Extrapolation of the dipolar liquid data to the ionic liquid regime suggests to us that it does not, but additional experiments are required before definite conclusions can be drawn.

Finally, the bianthryl reaction is rather different from the other two reactions studied here. Instead of time-resolved spectra resembling those expected for a two-state process, they are more similar to spectra of a nonreactive probe undergoing solvation. This difference in character is attributed to the fact that the LE → CT conversion, like solvation, is essentially a barrierless process in bianthryl. In such a case, reaction is not governed by simple rate laws and no unique time constant can be assigned. As did Barbara and co-workers[72,73] we defined reaction times in terms of the time-dependent intensities of the undifferentiated LE + CT emission band to approximately measure the survival probability of LE character. Doing so, we found that the (integral) times associated with electron transfer in bianthryl are approximately equal to the (integral) solvation times in ionic liquids. This near equality between reaction and solvation times in ionic liquids agrees nicely with the behavior reported previously in conventional dipolar solvents.[71,72,82] But the finding $\tau_{rxn} \cong \langle\tau_{solv}\rangle$ obtained here disagrees with conclusions of two prior studies of bianthryl in ionic liquids.[45−47] Comparison of TCSPC and femtosecond transient absorption data led Nagasawa et al.[45] to conclude that reaction is much faster than solvation. Preliminary fluorescence upconversion data presented here suggest that the difference in time resolution between the TCSPC and TA experiments probably accounts for some, but not all, of the disagreement. The substantial sub-picosecond component of the reaction observed in transient absorption experiments is not found in fluorescence measurements. Additional femtosecond fluorescence and absorption measurements will be needed to understand the reason for this discrepancy.

To summarize, the results in $BPAc^+$, bianthryl, and, with much less certainty, CVL suggest that ionic liquids behave as slow-moving versions of high-polarity conventional solvents in their effect on solvent-controlled electron-transfer reactions. At least in these low-barrier adiabatic processes, the distinction between solvation in dipolar versus ionic environments appears to be largely irrelevant. The situation might be different in the case of reactions with higher barriers. As shown by the modeling studies of Shim and Kim,[13,23] reactions with higher barriers sample only the faster portions of the solvation response, and in such cases the unusually distributed nature of ionic liquid solvation is likely to lead to more distinctive and liquid-specific results.

■ ASSOCIATED CONTENT

Ⓢ Supporting Information. Text, figures, and tables comparing the time-resolved Stokes shifts of bianthryl measured in the present study and those reported in refs 46 and 47. This information is available free of charge via the Internet at http://pubs.acs.org.

■ AUTHOR INFORMATION

Corresponding Author
*E-mail: maroncelli@psu.edu.

Present Addresses
[†]Department of Chemistry, IIT Indore, Madhyapradesh 452017, India.

■ ACKNOWLEDGMENT

We thank Naoki Ito for participating in some of the earliest portions of this work, Gary Baker for synthesis of several of the ionic liquids used here, and Gil Jones for preparing $BPAc^+$ and PAc^+. This work was funded by the Division of Chemical Sciences, Geosciences, and Biosciences, Office of Basic Energy Sciences of the U.S. Department of Energy through Grant DE-FG02-89ER14020.

■ REFERENCES

(1) Wasserscheid, P., Welton, T., Eds. *Ionic Liquids in Synthesis*, 2nd ed.; John Wiley and Sons: New York, 2008.
(2) *Ionic Liquids*; Kirchner, B., Ed.; Springer-Verlag: Berlin, 2009; Vol. 290.
(3) Plechkova, N. V.; Seddon, K. R. *Chem. Soc. Rev.* **2008**, *37*, 123.
(4) Wishart, J. F. *Energy Environ. Sci.* **2009**, *2*, 956.
(5) Zhou, F.; Liang, Y.; Liu, W. *Chem. Soc. Rev.* **2009**, *38*, 2590.
(6) Sun, P.; Armstrong, D. W. *Anal. Chim. Acta* **2010**, *661*, 1.
(7) Parvulescu, V. I.; Hardacre, C. *Chem. Rev.* **2007**, *107*, 2615.
(8) Stark, A. *Top. Curr. Chem.* **2009**, *290*, 41.
(9) Moniruzzaman, M.; Nakashima, K.; Kamiya, N.; Goto, M. *Biochem. Eng. J.* **2010**, *48*, 295.
(10) Hapiot, P.; Lagrost, C. *Chem. Rev.* **2008**, *108*, 2238.
(11) Tsuda, T.; Hussey, C. L. *Mod. Aspects Electrochem.* **2009**, *45*, 63.
(12) Lynden-Bell, R. M. *Electrochem. Commun.* **2007**, *9*, 1857.
(13) Shim, Y.; Kim, H. J. *J. Phys. Chem. B* **2007**, *111*, 4510.
(14) Poole, C. F. *J. Chromatogr., A* **2004**, *1037*, 49.
(15) Reichardt, C. *Green Chem.* **2005**, *7*, 339.
(16) Ferrer, B.; Garcia, H.; Schultz, K. P.; Nelsen, S. F. *J. Phys. Chem. B* **2007**, *111*, 13967.
(17) Jin, H.; Baker, G. A.; Arzhantsev, S.; Dong, J.; Maroncelli, M. *J. Phys. Chem. B* **2007**, *117*, 7291.
(18) Heitele, H. *Angew. Chem., Int. Ed. Engl.* **1993**, *32*, 359.
(19) Samanta, A. *J. Phys. Chem. Lett.* **2010**, *1*, 1557.
(20) Arzhantsev, S.; Jin, H.; Baker, G. A.; Maroncelli, M. *J. Phys. Chem. B* **2007**, *111*, 4978.
(21) Shim, Y.; Choi, M. Y.; Kim, H. J. *J. Chem. Phys.* **2005**, *122*, 044511.
(22) Kobrak, M. N. *J. Chem. Phys.* **2006**, *125*, 64502.
(23) Shim, Y.; Kim, H. J. *J. Phys. Chem. B* **2009**, *113*, 12964.
(24) Grote, R. F.; Hynes, J. T. *J. Chem. Phys.* **1980**, *73*, 2715.
(25) Gordon, C. M.; McLean, A. J. *Chem. Commun. (Cambridge, U. K.)* **2000**, 1395.
(26) McLean, A. J.; Muldoon, M. J.; Gordon, C. M.; Dunkin, I. R. *Chem. Commun. (Cambridge, U. K.)* **2002**, 1880.
(27) Skrzypczak, A.; Neta, P. *J. Phys. Chem. A* **2003**, *107*, 7800.
(28) Grampp, G.; Kattnig, D.; Mladenova, B. *Spectrochim. Acta A* **2006**, *63A*, 821.
(29) Paul, A.; Samanta, A. *J. Phys. Chem. B* **2007**, *111*, 1957.
(30) Vieira, R. C.; Falvey, D. E. *J. Phys. Chem. B* **2007**, *111*, 5023.
(31) Takahashi, K.; Sakai, S.; Tezuka, H.; Hiejima, Y.; Katsumura, Y.; Watanabe, M. *J. Phys. Chem. B* **2007**, *111*, 4807.
(32) Sarkar, S.; Pramanik, R.; Seth, D.; Setua, P.; Sarkar, N. *Chem. Phys. Lett.* **2009**, *477*, 102.
(33) Castner, E. W., Jr.; Margulis, C. J.; Maroncelli, M.; Wishart, J. F. *Annu. Rev. Phys. Chem.* **2011**, *62*, 85.
(34) Liang, M.; Kaintz, A.; Maroncelli, M. Unpublished results.
(35) Liu, H.; Liu, Y.; Li, J. *Phys. Chem. Chem. Phys.* **2010**, *12*, 1685.
(36) Dolidze, T. D.; Khoshtariya, D. E.; Illner, P.; Kulisiewicz, L.; Delgado, A.; van Eldik, R. *J. Phys. Chem. B* **2008**, *112*, 3085.
(37) Khoshtariya, D. E.; Dolidze, T. D.; van Eldik, R. *Chem.—Eur. J.* **2009**, *15*, 5254.
(38) Endres, F.; Hoefft, O.; Borisenko, N.; Gasparotto, L. H.; Prowald, A.; Al-Salman, R.; Carstens, T.; Atkin, R.; Bund, A.; Zein, E. A. S. *Phys. Chem. Chem. Phys.* **2010**, *12*, 1724.
(39) Hayes, R.; Warr, G. G.; Atkin, R. *Phys. Chem. Chem. Phys.* **2010**, *12*, 1709.
(40) Lockard, J. V.; Wasielewski, M. R. *J. Phys. Chem. B* **2007**, *111*, 11638.
(41) Jin, H.; Li, X.; Maroncelli, M. *J. Phys. Chem. B* **2007**, *111*, 13473.
(42) Jin, H.; Li, X.; Maroncelli, M. *J. Phys. Chem. B* **2010**, *114*, 11370.
(43) Blanco-Rodriguez, A. M.; Ronayne, K. L.; Zalis, S.; Sykora, J.; Hof, M.; Vlcek, A., Jr. *J. Phys. Chem. A* **2008**, *112*, 3506.
(44) Banerji, N.; Angulo, G.; Barabanov, I.; Vauthey, E. *J. Phys. Chem. A* **2008**, *112*, 9665.
(45) Nagasawa, Y.; Itoh, T.; Yasuda, M.; Ishibashi, Y.; Ito, S.; Miyasaka, H. *J. Phys. Chem. B* **2008**, *112*, 15758.
(46) Nagasawa, Y.; Oishi, A.; Itoh, T.; Yasuda, M.; Muramatsu, M.; Ishibashi, Y.; Ito, S.; Miyasaka, H. *J. Phys. Chem. C* **2009**, *113*, 11868.
(47) Khara, D. C.; Paul, A.; Santhosh, K.; Samanta, A. *J. Chem. Sci. (Bangalor)* **2009**, *121*, 309.
(48) Bose, S.; Wijeratne, A. B.; Thite, A.; Kraus, G. A.; Armstrong, D. W.; Petrich, J. W. *J. Phys. Chem. B* **2009**, *113*, 10825.
(49) Oum, K.; Lohse, P. W.; Ehlers, F.; Scholz, M.; Kopczynski, M.; Lenzer, T. *Angew. Chem., Int. Ed. Engl.* **2010**, *49*, 2230.
(50) Santhosh, K.; Banerjee, S.; Rangaraj, N.; Samanta, A. *J. Phys. Chem. B* **2010**, *114*, 1967.
(51) Santhosh, K.; Samanta, A. *J. Phys. Chem. B* **2010**, *114*, 9195.
(52) Khurmi, C.; Berg, M. A. *J. Phys. Chem. Lett.* **2010**, *1*, 161.
(53) Wu, H.; Wang, H.; Xue, L.; Shi, Y.; Li, X. *J. Phys. Chem. B* **2010**, *114*, 14420.
(54) Horng, M. L.; Gardecki, J. A.; Papazyan, A.; Maroncelli, M. *J. Phys. Chem.* **1995**, *99*, 17311.
(55) A helpful description of the low-lying excited states of bianthryl is provided in the recent computational work of Grozema et al.[97] In the gas phase, the LE (S_1) state is an excitonic mixture of two configurations having excitations localized on one of the two anthracene chromophores ($AA^* \leftrightarrow A^*A$). Above S_1 lie a pair of "charge-resonance" states involving equal mixtures of excitations from one anthracene ring to the other (A^+A^- and A^-A^+). In solution, asymmetric interactions with solvent molecules tend to localize the LE state to excitation on a single anthracene unit and to transform the nonpolar charge-resonance mixtures into true CT states in which a full electron is transferred between anthracene chromophores.
(56) Jones, G., II; Farahat, M. S.; Greenfield, S. R.; Gosztola, D. J.; Wasielewski, M. R. *Chem. Phys. Lett.* **1994**, *229*, 40.
(57) van Willigen, H.; Jones, G., II; Farahat, M. S. *J. Phys. Chem.* **1996**, *100*, 3312.
(58) Horng, M. L.; Dahl, K.; Jones, G.; Maroncelli, M. *Chem. Phys. Lett.* **1999**, *315*, 363.
(59) Lappe, J.; Cave, R. J.; Newton, M. D.; Rostov, I. V. *J. Phys. Chem. B* **2005**, *109*, 6610.
(60) Jones, G., II; Yan, D.; Hu, J.; Wan, J.; Xia, B.; Vullev, V. I. *J. Phys. Chem. B* **2007**, *111*, 6921.
(61) Karpiuk, J. *J. Phys. Chem. A* **2004**, *108*, 11183.
(62) Li, X.; Maroncelli, M. *J. Phys. Chem. A* **2010**(DOI: 10.1021/jp106240x).
(63) Karpiuk, J. *Phys. Chem. Chem. Phys.* **2003**, *5*, 1078.
(64) Karpiuk, J. *Phys. Chem. Chem. Phys.* **2005**, *7*, 4070.
(65) Schmidhammer, U.; Megerle, U.; Lochbrunner, S.; Riedle, E.; Karpiuk, J. *J. Phys. Chem. A* **2008**, *112*, 8487.
(66) Annapureddy, H. V. R.; Margulis, C. J. *J. Phys. Chem. B* **2009**, *113*, 12005.
(67) Hu, Z.; Margulis, C. J. *Proc. Natl. Acad. Sci. U. S. A.* **2006**, *103*, 831.
(68) Kimura, Y.; Fukuda, M.; Suda, K.; Terazima, M. *J. Phys. Chem. B* **2010**, *114*, 11847.
(69) Schneider, F.; Lippert, E. *Ber. Bunsen-Ges. Phys. Chem.* **1968**, *72*, 1155.

(70) Kahlow, M. A.; Kang, T. J.; Barbara, P. F. *J. Phys. Chem.* **1987**, *91*, 6452.
(71) Kang, T. J.; Kahlow, M. A.; Giser, D.; Swallen, S.; Nagarajan, V.; Jarzeba, W.; Barbara, P. F. *J. Phys. Chem.* **1988**, *92*, 6800.
(72) Kang, T. J.; Jarzeba, W.; Barbara, P. F.; Fonseca, T. *Chem. Phys.* **1990**, *149*, 81.
(73) Tominaga, K.; Walker, G. C.; Kang, T. J.; Barbara, P. F.; Fonseca, T. *J. Phys. Chem.* **1991**, *95*, 10485.
(74) Wortmann, R.; Elich, K.; Lebus, S.; Liptay, W. *J. Chem. Phys.* **1991**, *95*, 6371.
(75) Elich, K.; Kitazawa, M.; Okada, T.; Wortmann, R. *J. Phys. Chem. A* **1997**, *101*, 2010.
(76) Baumann, W.; Spohr, E.; Bischof, H.; Liptay, W. *J. Lumin.* **1987**, *37*, 227.
(77) Toublanc, D. B.; Fessenden, R. W.; Hitachi, A. *J. Phys. Chem.* **1989**, *93*, 2893.
(78) Piet, J. J.; Schuddeboom, W.; Wegewijs, B. R.; Grozema, F. C.; Warman, J. M. *J. Am. Chem. Soc.* **2001**, *123*, 5337.
(79) Schutz, M.; Schmidt, R. *J. Phys. Chem.* **1996**, *100*, 2012.
(80) Grabner, G.; Rechthaler, K.; Kohler, G. *J. Phys. Chem. A* **1998**, *102*, 689.
(81) Jurczok, M.; Plaza, P.; Martin, M.; Meyer, Y.; Rettig, W. *Chem. Phys.* **2000**, *253*, 339.
(82) Kovalenko, S. A.; Lustres, J. L. P.; Ernsting, N. P.; Rettig, W. *J. Phys. Chem. A* **2003**, *107*, 10228.
(83) Takaya, T.; Hamaguchi, H.-o.; Iwata, K. *J. Chem. Phys.* **2009**, *130*, 014501/1.
(84) Asami, N.; Takaya, T.; Yabumoto, S.; Shigeto, S.; Hamaguchi, H.-o.; Iwata, K. *J. Phys. Chem. A* **2010**, *114*, 6351.
(85) Subaric-Eitis, A.; Monte, C.; Roggan, A.; Rettig, W.; Zimmerman, P.; Heinze, J. *J. Chem. Phys.* **1990**, *93*, 4543.
(86) Tanaka, K.; Honma, K. *J. Phys. Chem. A* **2002**, *106*, 1926.
(87) Jones, G.; Farahat, M. S.; Greenfield, S. R.; Gosztola, D. J.; Wasielewski, M. R. *Chem. Phys. Lett.* **1994**, *229*, 40.
(88) Bell, F.; Waring, D. H. *J. Chem. Soc.* **1949**, 267.
(89) (a) Jin, H.; O'Hare, B.; Dong, J.; Arzhantsev, S.; Baker, G. A.; Wishart, J. F.; Benesi, A.; Maroncelli, M. *J. Phys. Chem. B* **2008**, *112*, 81. (b) Jin, H.; O'Hare, B.; Dong, J.; Arzhantsev, S.; Baker, G. A.; Wishart, J. F.; Benesi, A. J.; Maroncelli, M. *J. Phys. Chem. B* **2010**, *115*, 1333.
(90) Heitz, M. P.; Maroncelli, M. *J. Phys. Chem. A* **1997**, *101*, 5852.
(91) Maroncelli, M.; Fleming, G. R. *J. Chem. Phys.* **1987**, *86*, 6221.
(92) Shimizu, K.; Costa, G. M. F.; Padua, A. A. H.; Rebelo, L. P. N.; Canongia, L. J. N. *J. Mol. Struct. (THEOCHEM)* **2010**, *946*, 70.
(93) Koti, A. S. R.; Krishna, M. M. G.; Periasamy, N. *J. Phys. Chem. A* **2001**, *105*, 1767.
(94) Del Sesto, R. E.; Corley, C.; Robertson, A.; Wilkes, J. S. *J. Organomet. Chem.* **2005**, *690*, 2536.
(95) Fee, R. S.; Maroncelli, M. *Chem. Phys.* **1994**, *183*, 235.
(96) Zhang, X.; Liang, M.; Ernsting, N. P.; Maroncelli, M. *J. Phys. Chem. B* **2011**manuscript in preparation.
(97) Grozema, F. C.; Swart, M.; Zijlstra, R. W. J.; Piet, J. J.; Siebbeles, L. D. A.; van Duijnen, P. T. *J. Am. Chem. Soc.* **2005**, *127*, 11019.
(98) Tariq, M.; Forte, P. A. S.; Gomes, M. F. C.; Lopes, J. N. C.; Rebelo, L. P. N. *J. Chem. Thermodyn.* **2009**, *41*, 790.
(99) Matsumoto, H.; Kageyama, H.; Miyazaki, Y. *Chem. Commun. (Cambridge, U. K.)* **2002**, 1726.
(100) Ito, N.; Arzhantsev, S.; Maroncelli, M. *Chem. Phys. Lett.* **2004**, *396*, 83.